POWER CONVERSION UNIT STUDIES FOR THE NEXT GENERATION NUCLEAR PLANT COUPLED TO A HIGH -TEMPERATURE STEAM ELECTROLYSIS FACILITY

A Thesis

by

ROBERT BUCKNER BARNER

Submitted to the Office of Graduate Studies of
Texas A&M University
in partial fulfillment of the requirements for the degree of

MASTER OF SCIENCE

December 2006

Major Subject: Nuclear Engineering

POWER CONVERSION UNIT STUDIES FOR THE NEXT GENERATION NUCLEAR PLANT COUPLED TO A HIGH-TEMPERATURE STEAM ELECTROLYSIS FACILITY

A Thesis

by

ROBERT BUCKNER BARNER

Submitted to the Office of Graduate Studies of
Texas A&M University
in partial fulfillment of the requirements for the degree of

MASTER OF SCIENCE

Approved by:

Chair of Committee, Yassin Hassan
Committee Members, William Marlow
Kalyan Annamalai
Head of Department, William Burchill

December 2006

Major Subject: Nuclear Engineering

ABSTRACT

Power Conversion Unit Studies for the Next Generation Nuclear Plant

Coupled to a High-temperature Steam Electrolysis Facility. (December 2006)

Robert Buckner Barner, B.S., Texas A&M University

Chair of Advisory Committee: Dr. Yassin Hassan

The Department of Energy and the Idaho National Laboratory are developing a Next Generation Nuclear Plant (NGNP) to serve as a demonstration of state-of-the-art nuclear technology. The purpose of the demonstration is two fold: 1) efficient low cost energy generation and 2) hydrogen production. Although a next generation plant could be developed as a single-purpose facility, early designs are expected to be dual-purpose. While hydrogen production and advanced energy cycles are still in their early stages of development, research towards coupling a high temperature reactor, electrical generation and hydrogen production is under way. Many aspects of the NGNP must be researched and developed to make recommendations on the final design of the plant. Parameters such as working conditions, cycle components, working fluids, and power conversion unit configurations must be understood.

Three configurations of the power conversion unit were modeled using the process code HYSYS; a three-shaft design with 3 turbines and 4 compressors, a combined cycle with a Brayton top cycle and a Rankine bottoming cycle, and a reheated cycle with 3 stages of reheat were investigated. A high temperature steam electrolysis hydrogen production plant was coupled to the reactor and power conversion unit by means of an intermediate heat transport loop. Helium, CO_2, and an 80% nitrogen, 20% helium mixture (by weight) were studied to determine the best working fluid in terms cycle efficiency and development cost. In each of these configurations the relative heat exchanger size and turbomachinery work were estimated for the different working fluids.

Parametric studies away from the baseline values of the three-shaft and combined cycles were performed to determine the effect of varying conditions in the cycle. Recommendations on the optimal working fluid for each configuration were made.

The helium working fluid produced the highest overall plant efficiency for the three-shaft and reheat cycle; however, the nitrogen-helium mixture produced similar efficiency with smaller component sizes. The CO_2 working fluid is recommend in the combined cycle configuration.

DEDICATION

To my wife

ACKNOWLEDGMENTS

I would first like to thank Dr. Yassin Hassan for his support and providing me the opportunity to conduct this research. I would also like to thank my committee members Dr. William Marlow and Dr. Kaylan Annamalai for serving on my committee and providing support during my research.

Next, I would like to thank Dr. Chang Oh for giving me the opportunity to work with him at the Idaho National Lab. I extend my gratitude to those at the Idaho National Laboratory who provided me with their guidance and patience: Cliff Davis and Mike McKellar.

Thank you to my wife, Scottie, for her support and encouragement during my research and allowing me to continue my graduate studies. Finally I would like to thank my parents, Jerry and Elizabeth, and the rest of my family for their support during my research.

TABLE OF CONTENTS

Page

LIST OF TABLES

TABLE Page

LIST OF FIGURES

FIGURE Page

I. INTRODUCTION

As the world grows and becomes more modern, so does the worlds dependency on energy. New and renewable options must be investigated to meet the ever growing demand for electricity. Nuclear power is poised to meet this demand with advanced designs that are environmentally clean and increasingly safer. Six next generation or Gen IV reactor designs have postulated; Gas-cooled Fast Reactor (GFR), Lead-cooled Fast Reactor (LFR), Molten Salt Reactor (MSR), Sodium-cooled Fast Reactor (SFR), Supercritical-water-cooled Reactor (SCWR) and the Very-high-temperature Reactor (VHTR). An international effort to develop these new technologies is under way and advances in materials are allowing increased operating temperatures and pressures.

The GFR will use a helium coolant in a direct cycle similar to that of the Pebble-bed Modular Reactor and the Gas-turbine Modular Helium Reactor. The primary difference will be that the GFR would be a breeder reactor. The LFR continues from current breeder reactors which use molten metal coolant and would be used with either a lead or lead-bismuth alloy as the coolant. The MSR utilizes a liquid salt coolant such as sodium and boasts high fuel burn up, safe operation and proliferation resistance as compared to other Gen IV designs. The SFR is the most popular breeder design but development has been lagging due to interest in other Gen IV designs especially the VHTR. The SCWR continues from current light water reactor (LWR) designs such as the pressurized water reactor (PWR) and boiling water reactor (BWR). Advantages of the cycle include familiarity and lower construction and operating costs. Finally, the VHTR would operate at very high temperatures which allow for both electrical and hydrogen production[1].

The Department of Energy and the Idaho National Laboratory are developing a Next Generation Nuclear Plant (NGNP) to serve as a demonstration of state-of-the-art nuclear technology. The purpose of the demonstration is two fold 1) efficient low cost energy generation and 2) hydrogen production. Although a next generation plant could

---

This thesis follows the style and format of *Nuclear Technology*.

be developed as a single-purpose facility, early designs are expected to be dual-purpose. While hydrogen production and advanced energy cycles are still in its early stages of development, research towards coupling a high temperature reactor, electrical generation and hydrogen production is under way. Many aspects of the NGNP must be researched and developed in order to make recommendations on the final design of the plant. Parameters such as working conditions, cycle components, working fluids, and power conversion unit (PCU) configurations must be understood.

In order to accomplish the dual purpose facility the reactor must be coupled to a PCU as well as the hydrogen production plant. Davis et al. describes 7 different configuration for the coupling of these systems including direct and indirect cycles, parallel and series configurations of the PCU and the intermediate heat transport loop used to transport process heat from the reactor to the hydrogen production facility[2]. An intermediate heat transport loop (IHTL) delivering 50MW of process heat to the hydrogen production plant has been recommend[3]. Several estimations of the required separation distance between the nuclear and hydrogen process plant vary have been postulated. For example, Sochet et al. recommended 500 m for the High-Temperature Reactor while Smith et al. recommended a separation distance of from 60 to 120 m for the NGNP and the hydrogen production plant[4,5]. Davis et al. investigated the possibility of helium and molten salts in the IHTL[2].

The thermal efficiency of the power conversion unit is paramount to the success of this next generation technology. Current light water reactor systems have a modest efficiency of 30-35%, while current estimates of the gas turbine modular helium reactor (GT-MHR) are 48%[6]. The GT-MHR power conversion unit consists of a gas turbine, recuperator, precooler, low-pressure compressor, intercooler and a high-pressure compressor in a direct cycle. AREVA is also investigating a very high temperature reactor design utilizing an indirect combined cycle PCU[7]. Initial estimates of the combined cycle show an efficiency advantage over a direct cycle similar to the GT-MHR of 1-1.5%[7]. By using a liquid-metal or molten-salt primary coolant, the possibility of using multiple reheating stages could increase the thermal efficiency[8]. Peterson

reports, that with reactor outlet temperatures of 800°C, a thermal efficiency of 54% could be achieved[8].

This paper investigates various PCU configurations coupled to a High Temperature Steam Electrolysis (HTSE) plant by means of an intermediate heat transport loop. The key issues that are addressed in this document are: (1) PCU configuration options, (2) coupling of the HTSE to the reactor (3) working fluids in the PCU and IHTL (4) efficiency optimization and (5) component sizing.

The commercial process code HYSYS was used to model the facility and determine the balance of plant (BOP) for the entire system. A three-shaft Brayton cycle design with 3 turbines and 4 compressors, a combined cycle with a Brayton top cycle and a Rankine bottoming cycle, and a reheated Brayton cycle with 3 stages of reheat were investigated. An intermediate heat transport loop for transporting heat to the HTSE plant was used. This intermediate heat transport loop was modified from configuration 6 from a report by Davis et al. and the HTSE plant was adapted from work by Stoots et al.[2,9]

Helium, CO_2, and an 80% nitrogen, 20% helium mixture (by weight) were studied to determine the best PCU working fluid in terms cycle efficiency and development cost. Relative component sizing information was estimated for the different working fluids. The relative size of the turbomachinery was measured by comparing the power input/output of the component. For heat exchangers, a printed circuit heat exchanger (PCHE) or tube-in-shell design was assumed and the volume was computed and compared. Parametric studies away from the baseline values of the systems were performed to determine the effect of varying conditions in the cycle giving insight into the sensitivity of these cycles to various operating conditions. The parametric studies were carried out on reactor outlet temperature, mass flow in the PCU, pressure in the PCU, and a turbine cooling system.

II. METHODS*

This section describes the methods that were used in coupling the HTSE plant to the reactor, determining the overall efficiency, component sizes and cycle sensitivity to varying working conditions. The design configurations that were studied are described in Section III.A. The working fluids selection process is explained in Section III.B. The optimization process that was used to determine maximum cycle efficiency is illustrated in Section III.C. Section III.D establishes the processes for determining component sizes. Finally the parametric studies were performed on the various PCU configurations and are described in Section III.E.

A. Design Configuration

The design of the NGNP power conversion unit is demonstrated using three-shaft, combined and reheated cycle designs to better understand the consequences of various cycle configurations. Both direct and indirect cycles have been postulated for use in the NGNP. The direct cycle eliminates the need for an intermediate heat exchanger (IHX) between the primary and secondary loop and therefore has a higher efficiency. However this poses increased development risk due to no separation between the reactor and cycle components. An indirect cycle has decreased risk and only a small decrease in efficiency while also allowing for the use of CO_2 as a working fluid in the secondary side. Furthermore, the Independent Technology Review Group recommended the use of an indirect cycle for the NGNP[10]. For these reason an indirect cycle was used in this study.

The NGNP reactor was assumed to produce 600 MW of thermal power with a 900 °C outlet temperature and a nominal reactor pressure of 7 MPa using a helium coolant on the primary side[11]. The nominal rise in fluid temperature across the core was assumed to

* Part of this section is reprinted with permission from "Evaluation of Working Fluids in an Indirect Combined Cycle in a Very High Temperature Gas-Cooled Reactor" by Chang Oh, Robert Barner, Cliff Davis and Steve Sherman, 2006. *Nuclear Technology*, 156, 1-10. Copyright 2006 by American Nuclear Society, La Grange Park, IL.

be 400 °C, based on the point design MacDonald et al.[12]. The primary side of the plant was kept constant for the three-shaft and combined cycles, however for the reheat option the primary side was modified to take advantage of the cycle. The primary side working conditions for the three-shaft and combined are summarized in Table I.

TABLE I
Summary of primary working conditions for three-shaft and combined cycles.

Parameter	Nominal Value
Thermal power, MW	600
Inlet temperature, °C	500
Inlet Pressure, MPa	7.05
Outlet temperature, °C	900
Outlet pressure, MPa	7
IHX pressure drop, MPa	0.05
Mass Flow, kg/s	289
Working fluid	He

In the reheated cycle the primary side was altered to produce a more realistic model of the cycle. The reactor inlet temperature must be raised to take advantage of the reheat option. This was done by raising the mass flow through the primary side. The additional intermediate heat exchangers need for the reheat cycle make the use of helium in the primary side infeasible. The additional pressure drop incurred by the heat exchangers offsets the benefits of reheating. Therefore to take advantage of reheat a molten salt was used as the primary working fluid, which has a very small pressure drop relative to helium, making the use of reheating feasible[8]. Flibe which is composed of 66% LiF and 34% BeF_2, by weight, was used for this study[8]. Flibe is an incompressible liquid and the pressure drop for this fluid is very low and was assumed to be negligible. The primary side working conditions for the reheat cycle are summarized in Table II.

The NGNP is envisioned to be a demonstration plant for hydrogen production and electrical generation. In order for hydrogen production to be possible, process heat from

the reactor must be transported to the hydrogen production plant. To accomplish this, an intermediate heat transport loop was added to the NGNP design. The intermediate heat transport loop was assumed to be the same for all configurations and was adapted from the work of Davis et al. and consists of a heat transport loop heat exchanger (HTLHX) between the reactor and the IHTL, piping to the hydrogen process plant, a series of heat exchanger between the loop and hydrogen process plant called the process heat exchangers (PHX), and a circulator[2]. The intermediate heat transport loop was assumed to receive 50 MW of thermal power[3]. Estimations of the required separation distance between the nuclear and hydrogen process plant vary considerable. For example, Sochet et al. recommended 500 m for the High-Temperature Reactor while Smith et al. recommended a separation distance of from 60 to 120 m for the NGNP and the hydrogen production plant[4,5]. For this analysis, a nominal value of 90 m was used. Both helium and liquid salts were considered as working fluids for the IHTL. The liquid salt $NaBF_4$-NaF in molar concentrations of 92% and 8% was considered for its low freezing temperature of 385 °C. The use of this liquid salts can potentially increase the heat transfer and reduce the pumping power; however it also introduces material problems such as compatibility and freezing[2]. The working conditions for each working fluid used in that loop are summarized in Table III.

TABLE II
Summary of primary working conditions for reheated cycle.

Parameter	Nominal Value
Thermal power, MW	600
Pressure, MPa	0.1013
Reactor outlet temperature, °C	900
IHX pressure drop, MPa	~0

In this analysis two configurations were used for the placement of the intermediate heat transport loop. The first configuration was used in the three-shaft and

combined cycle models and assumes the HTLHX is placed in parallel with the PCU on the secondary side. In this configuration, which is illustrated in Figure 1, the IHX cold-side outlet fluid is split, with most going towards the PCU and the remainder going towards the HTLHX. A small circulator is required to compensate for the pressure loss across the HTLHX and allow the fluid streams to mix downstream of the PCU. The reheat option did not allow for this configuration so a new configuration was develop in which the HTLHX is placed in parallel with the intermediate heat exchangers in primary loop as illustrated in Figure 2.

TABLE III
Working conditions in the intermediate heat transport loop.

Parameter	**Nominal Value**	
	He	**$NaBF_4$-NaF**
Power, MW	50.4	49.3
Heat Loss, MW	1.79	1.79
Outlet temperature of HTLHX, °C	875.1	875.1
Pressure drop, kPa	139.0	5.0
Pressure, MPa	2	2
Mass Flow, kg/s	27.5	94.8

The coupling of the IHTL to the HTSE was accomplished by means of three PHX's. Figure 3 details the configuration of the PHX's in the IHTL in which two heat exchangers in parallel are followed by one heat exchanger in series. This configuration was chosen to deliver high inlet temperatures on the hot side of the first two heat exchangers where high cold side outlet temperatures are needed for the HTSE plant. The third heat exchanger however, does not require high cold side outlet temperatures and the hot side inlet temperature from the outlet of the prior heat exchangers is sufficient for heating the cold side fluid.

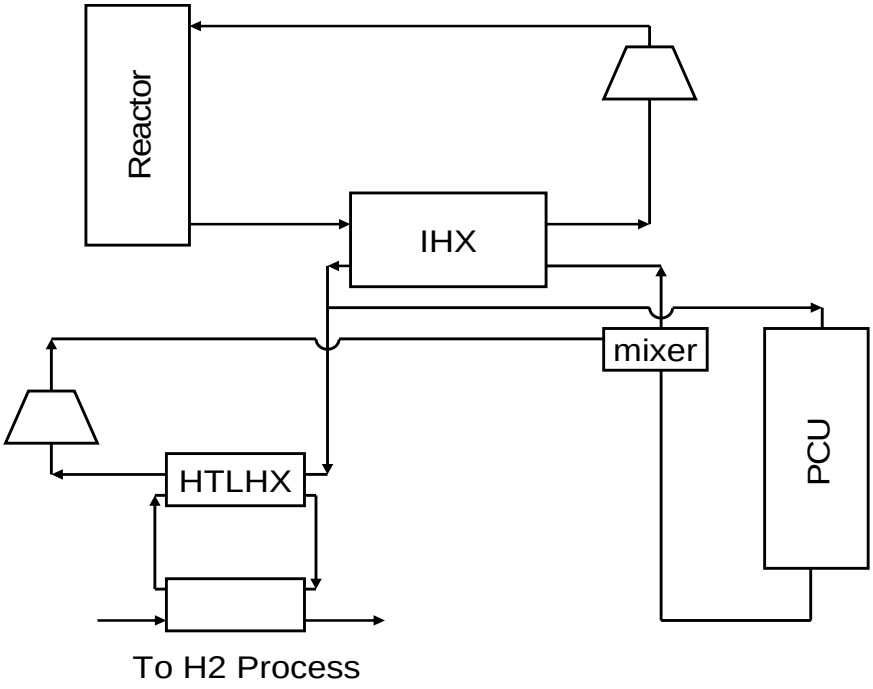

Figure 1. Schematic of parallel HTLHX option for the three-shaft and combined cycle configurations.

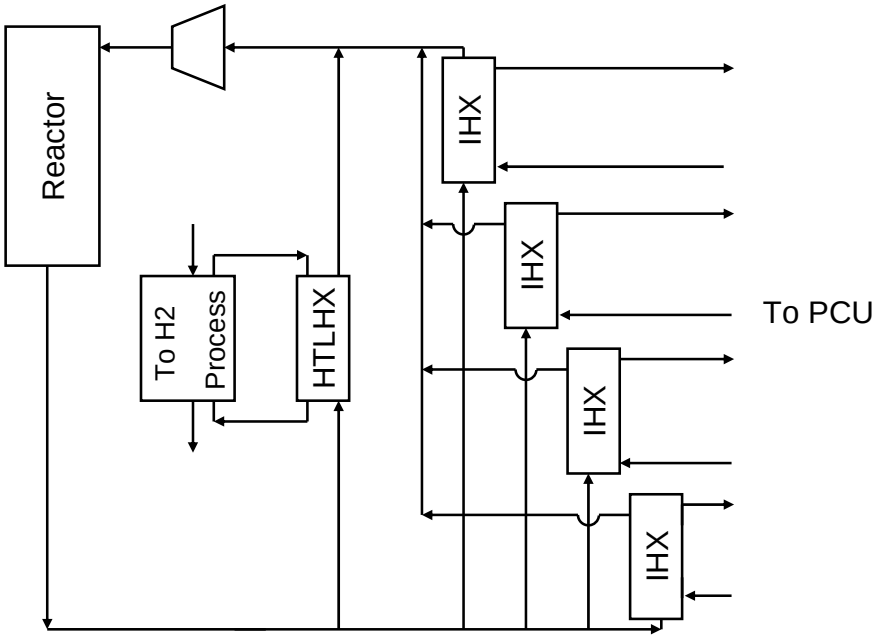

Figure 2. Schematic of HTLHX configuration when using the reheat option.

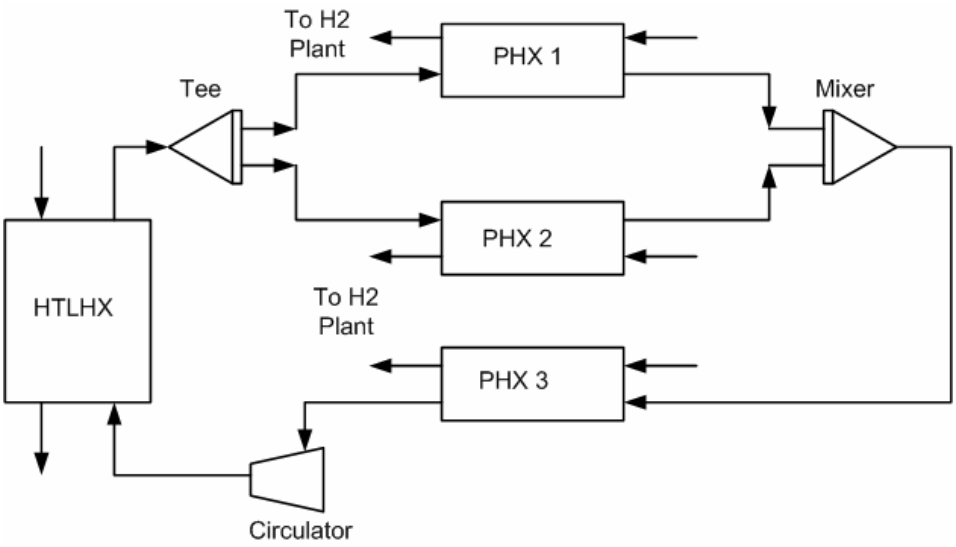

Figure 3. IHTL process heat exchanger configuration.

1. Three-Shaft Cycle

A three-shaft design was originally envisioned for the baseline PCU configuration of the NGNP project. This configuration is illustrated in Figure 4 and consists of; (1) a primary loop (2) an intermediate heat transport loop in parallel with (3) the PCU with three turbines (high pressure turbine, low pressure turbine and power turbine), 4 compressors (low pressure compressor, medium pressure compressor 1, medium pressure compressor 2, and high pressure compressor) 1 precooler, 3 intercoolers and a recuperator. The high pressure turbine is connected by one shaft to power the high and one medium pressure compressors. The medium pressure turbine is connected by a second shaft to power the remaining compressors. Finally the low pressure turbine is on a third shaft which power a generator for electricity production. By using intercooling between the compression stages the average temperature at which heat is rejected from the system is reduced. However as more heat exchangers are added to the system the

pressure drop increases as well as the cost. There is a trade-off between the efficiency gain due to decreasing the average rejection temperature and efficiency loss due to increase pressure drop. At some point the pressure drop overwhelms the temperature increase and an efficiency loss is realized. Chang et al. preformed studies to determine the effects of additional intercooling stages on cycle efficiency and found that after three stages of intercooling the increased efficiency due to an additional intercooler was offset by the additional pressure loss to the system[13].

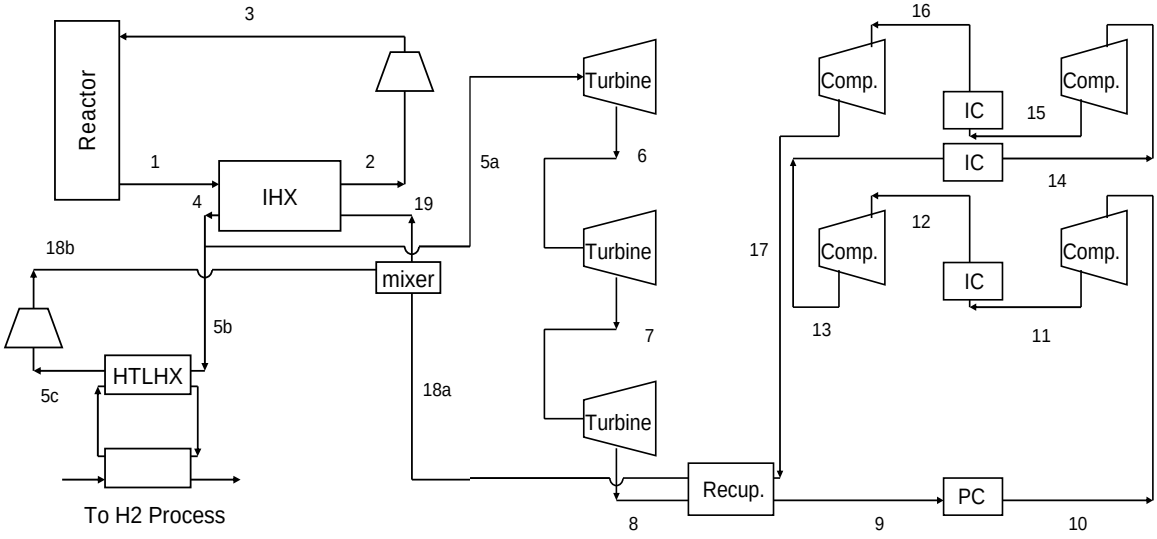

Figure 4. Schematic of three-shaft cycle PCU configuration.

2. Combined Cycle

A combined cycle was originally envisioned by Framatome ANP for the NGNP project[6]. This configuration is illustrated in Figure 5 and consists of; (1) a primary loop (2) and an intermediate heat transport loop in parallel with (3) a PCU with 1 gas turbine, 1 gas compressor, a steam generator, a steam turbine, a condenser, and a pump. The gas turbine and compressor are on the same shaft along with a generator for electricity production while the steam generator and pump are on a second shaft. In a combined

cycle the use of a Rankine bottoming cycle has the potential of increasing the plant efficiency beyond that of a conventional high-temperature gas cooled reactors[7]. The Rankine cycle also decreases the cost to produce electrical power by taking advantage of existing technologies and reducing development risk[7].

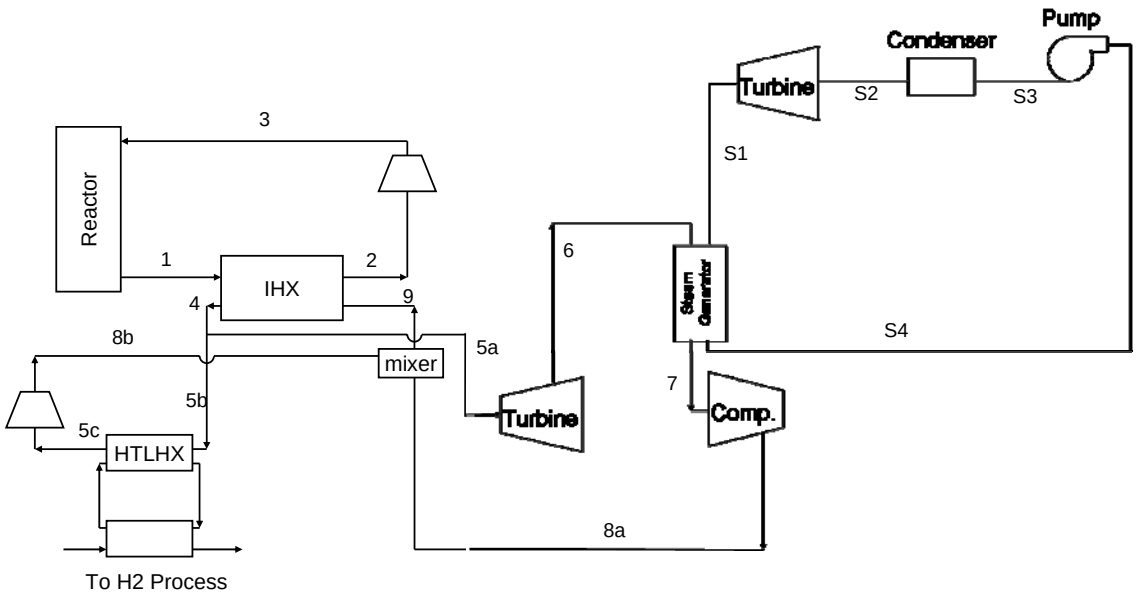

Figure 5. Schematic of the combined cycle PCU configuration.

3. Reheated Cycle

The reheat cycle, illustrated in Figure 6 consists of; (1) a primary loop with 4 IHX's (2) an intermediate heat transport loop in series with the IHX's on the primary loop, (3) the PCU with four turbines (high pressure turbine, medium pressure turbine 1, medium pressure turbine 2, low pressure turbine), 4 compressors (low pressure compressor, medium pressure compressor 1, medium pressure compressor 2, and high pressure compressor) 1 precooler, 3 intercoolers and a recuperator. Each turbine is connected to one compressor and a generator by a shaft.

A reheating option can increase the efficiency of a cycle by increase the average temperature at which heat is added to the system. This effectively increases the

equivalent Carnot temperature for the cycle; however the problem of losses due to increased pressure drops works to decrease efficiency. To help alleviate the effects of pressure drop a liquid salt working fluid can be used in the primary side of the cycle[8].

To optimize the efficiency improvement from reheat the inlet and outlet temperatures for the turbines should be kept the same[14]. For a cycle employing an ideal gas, an equal split of total pressure ratio is ideal. Since helium, nitrogen and CO_2 are very close to ideal gases in the temperature and pressure range used in the turbines, this same assumption was made in this study.

When using the reheat option, up to 4 intermediate heat exchangers could be used. This leads to an increase in pumping power required as compared to a single IHX configuration. The mass flow rate must also be raised for the reheat option to be applicable, also leading to a higher pumping power. To decrease the pumping power required for a helium coolant, a molten salt, Flibe, was studied as the working fluid[8].

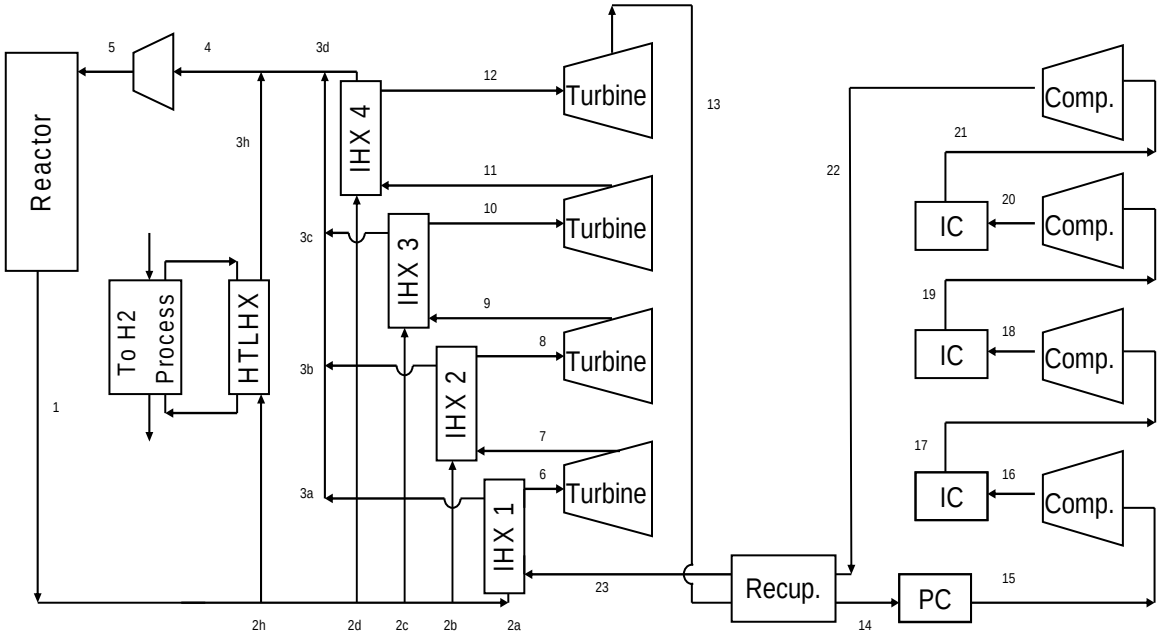

Figure 6. Schematic of reheated cycle PCU configuration.

4. HTSE Hydrogen Plant

To act as a dual purpose facility, a power conversion unit as well as a hydrogen production plant must be coupled to the reactor. In this study a baseline High Temperature Steam Electrolysis plant will be coupled to the reactor by means of the IHTL. The HTSE model used here was adapted from the work done by Stoots et al.[9]. A model of the HTSE operations was developed at Idaho National Laboratory that includes all of the components that are actually present in a HTSE plant including pumps, compressors, heat exchangers, expanders and the electrolyzer. A one dimensional electrolyzer model was developed for the HYSYS modeling code. A comparison of this model with a fully 3-D computational fluid dynamic model and experimental results was done by O'Brian et al.[15].

Referring to Figure 7, the process water enters on the left. The water is then pumped up to the operating pressure of 5 MPa. The efficiency of the pumps and circulators is assumed to be 75%. This water is then combined with water condensate returned from the hydrogen/water product stream. This stream then enters the low temperature recuperator. The pressure drop through the heat exchangers is assumed to be 20 kPa. From there the steam is further heated by PHX 3. Upon leaving PHX 3 the steam is mixed with hydrogen from the product stream by a recirculator which works to overcome the pressure drops in the system. A mole fraction of 90% water and 10% hydrogen is maintained in this model. This hydrogen helps to maintain reducing conditions at the electrolysis stack to prevent oxidation. The mixed stream then enters the high temperature recuperator which takes advantage of the high temperature outlet from the electrolysis stack. The hydrogen/water stream is then heated to the operating temperature for the electrolysis stack, in this case 827 °C, in PHX 1.

The electrolyzer has another inlet stream which contains the sweep gas. This is used to sweep away the oxygen from the electrolysis process. A steam sweep gas is used in this model and enters the plant in the middle-bottom of Figure 7. It is first pumped up to operating pressure and then heated in a heat exchanger using the hot sweep outlet from

the electrolyzer. Before it enters the electrolysis stack it is heated to the operating temperature of 827 °C in PHX 2.

Upon leaving the electrolyzer, the product stream is 90% hydrogen and 10% water. This then passes through the high and low temperature recuperators. The steam condensate is then separated from the hydrogen and recycled back into the system. After leaving the electrolyzer, the sweep gas enters the recuperator to preheat the sweep inlet. The sweep outlet contains approximately 55% water and 45% oxygen. It is then partially separated before entering an expander to recuperate some of the power. The expander has an efficiency of 80%. Finally the sweep stream is further separated and high purity oxygen and water are produced.

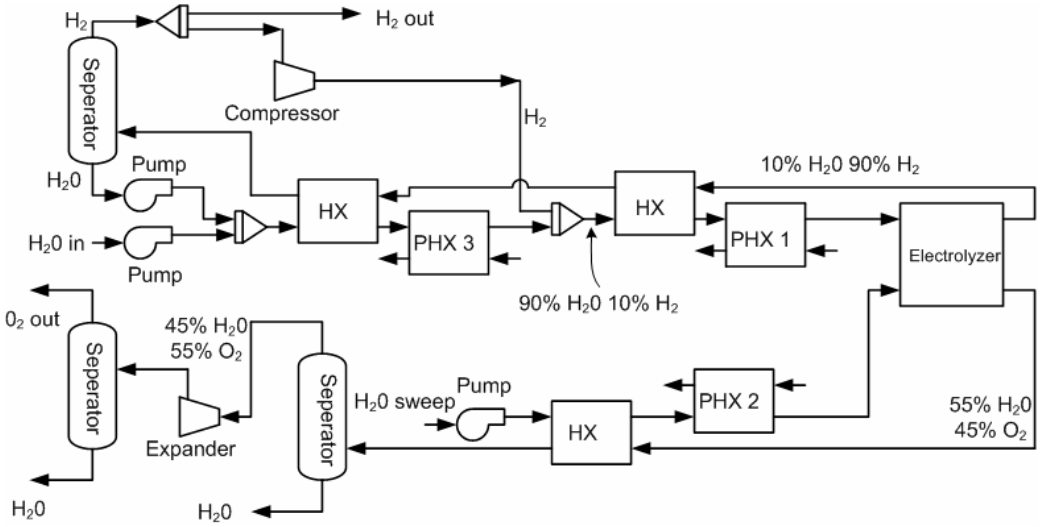

Figure 7. Schematic of HTSE process.

The model developed by Stoots et al. was originally envisioned for a 300 MW HTSE plant[9]. However, under the assumption of ~50 MW process heat, a 300 MW plant was not possible. Therefore the plant was scaled down to meet the needs of that assumption. To do this, the balance of plant must still work and key working condition

such as stream compositions and electrolyzer inlet temperature must remain constant. This was accomplished by reducing the mass flow of the inlet process stream and the sweep stream while keeping the compositions and temperatures constant. The electrical power to the electrolyzer was reduced from 292 MW to 234.4 MW and 198.8 MW for the helium and molten salt IHTL working fluids, respectively. This was done to account for the smaller mass flow rate and to keep an outlet composition of 90% hydrogen and 10% water.

B. Working Fluids

Helium was used as the working fluid in the primary side of the NGNP for the three-shaft and combined cycles and Flibe was used for the reheated cycle. Helium, CO_2, and 80% nitrogen, 20% helium mixture (by weight) were studied to determine the best secondary side working fluid in terms cycle efficiency and development cost. Helium is a well understood fluid and has been used in numerous studies pertaining to nuclear power. CO_2 does possess some advantages over helium such as a higher density allowing for smaller velocities than helium for the same pressure drops[16]. Despite the lower specific heat, the volumetric flow rates are smaller for CO_2 than for a helium cycle generating equivalent power, making the turbomachinery sizes smaller for CO_2[16]. A nitrogen-helium mixture for the working fluid was initially investigated for a combined cycle[7]. Helium and a molten salt ($NaBF_4$-NaF) were recommended for the working fluid of the IHTL and were further investigated here[2].

The Peng-Robinson (1976) equation of state was used by HYSYS to calculate the fluid properties of the helium, CO_2 and nitrogen-helium mixture. To calculate the viscosity and thermal conductivity of the fluids HYSYS uses a modified National Bureau of Standards method developed by Ely and Hanley[17]. The values calculated by HYSYS were compared to the NIST database and the properties calculated by HYSYS for helium and nitrogen were not in agreement[18]. HYSYS Simulation Basis recommends these values being entered as tabulated data for helium for more accurate properties[17].

Therefore, the viscosity and thermal conductivity data for helium and nitrogen from the NIST database were entered in to HYSYS. HYSYS then performs a regression on the tabular data to get the fluid properties. HYSYS does not contain the properties of the molten salt used in the primary side of the reheat cycle or the IHTL. This was overcome by entering the fluid properties of the materials in tabular form and HYSYS performing a regression. For the water and steam used in the Rankine cycle HYSYS uses ASME tables[17].

C. Efficiency Optimization

Using the limiting conditions established in Table I through Table VI the cycles were modeled and optimized in HYSYS. To calculate the efficiency, the spreadsheet function of HYSYS was used and values from the cycle were import from the model. The efficiency of the power conversion unit was calculated as follows

$$\eta_{PCU} = \frac{\Sigma W_T - \Sigma W_C - \Sigma W_{CIR}}{Q_{th} - Q_{IHTL}}, \quad (1)$$

where ΣW_T is the total turbine power, ΣW_C is the total compressor workload, ΣW_{CIR} is the circulator workload in the primary and secondary side, Q_{th} is the reactor thermal power and Q_{IHTL} is the heat delivered to the IHTL through the HTLHX. The efficiency of the overall cycle including the HTSE plant was calculated as follows

$$\eta_{overall} = \frac{\Sigma W_T - \Sigma W_C - \Sigma W_{CIR} + \Sigma W_{H2} - Q_{EL} + Q_{H2}}{Q_{th}}, \quad (2)$$

where ΣW_{H2} is the workload in the HTSE plant, Q_{EL} is the power supplied to the electrolyzer, Q_{H2} is the lower heating value of the produced hydrogen and Q_{th} is the reactor thermal power.

A model to solve for the effectiveness ε of a heat exchanger is not defined in HYSYS and had to be developed. The effectiveness of a heat exchanger is defined as the ratio of the actual heat transfer rate to the maximum heat transfer rate. The spreadsheet function was used and the following equations were input

$$\varepsilon = \frac{q}{q_{\max}}, \tag{3}$$

$$q_{\max} = C_{mim}(T_{h,i} - T_{c,i}), \tag{4}$$

where C_{min} refers to the smaller of C_{hot} or C_{cold} which are defined as

$$C_{hot} = c_{p,hot}\dot{m}_{hot}, \tag{5}$$

$$C_{cold} = c_{p,cold}\dot{m}_{cold}. \tag{6}$$

The log mean temperature difference (LMTD) and the minimum approach were calculated by HYSYS and used to determine heat exchanger performance. The effectiveness, LMTD, and minimum approach served as limits to the allowable working conditions within the cycle. An acceptable effectiveness, LMTD and minimum approach for each heat exchanger were determined and the working conditions were set to take advantage of these limits in order to maximize efficiency. The pressure for each heat exchanger was calculated using the methods described in Section D.

The polytropic efficiency of the turbomachinery was used for efficiency calculation rather than the isentropic efficiency. The polytropic efficiencies for the turbines and the compressors were assumed to be 92% and 90%, respectively. These values are representative of expected efficiency that will be available for the NGNP project. For expansion the efficiency is calculated from

$$\frac{T_{0,ex}}{T_{0,in}} = \left(\frac{P_{0,ex}}{P_{0,in}} \right)^{\left(\frac{R}{C_p} \eta_{p,e} \right)}, \tag{7}$$

where T_0 is the stagnation temperature, P_0 is the stagnation pressure, R is the gas constant, C_p is the specific heat, $\eta_{p,e}$ is the polytropic efficiency and the subscripts *in* and *ex* refer to the inlet and outlet conditions. For compression, the efficiency is calculated as

$$\frac{T_{0,ex}}{T_{0,in}} = \left(\frac{P_{0,ex}}{P_{0,in}} \right)^{\left(\frac{R}{C_p} \frac{1}{\eta_{p,c}} \right)}. \tag{8}$$

Once the working conditions and limits were set the cycle pressure ratios were optimized. The combined cycle allowed for the additional optimization of the mass split between the PCU and.

TABLE IV
Cycle conditions for three-shaft configuration.

Parameter	Nominal Value
IHX cold-side outlet temp, °C	885
IHX effectiveness limit	<97%
IHX temperature pinch limit, °C	5
IHX LMTD, °C	15
Compressor outlet pressure, MPa	7.05
Precooler outlet temperature, °C	30
Recuperator effectiveness	95%
HTLHX effectiveness limit	<97%
HTLHX temperature pinch limit, °C	5
HTLHX LMTD, °C	27

TABLE V
Cycle conditions for combined configuration.

Parameter	Nominal Value
IHX cold-side outlet temp, °C	885
IHX effectiveness limit	<97%
IHX temperature pinch limit, °C	5
IHX LMTD, °C	15
Compressor outlet pressure, MPa	7.05
HTLHX effectiveness limit	<97%
HTLHX temperature pinch limit, °C	5
HTLHX LMTD, °C	27
Steam generator temperature pinch, °C	5
Steam turbine outlet quality	>85%
Steam turbine outlet pressure, kPa	20
Pump outlet pressure, MPa	15

TABLE VI
Cycle conditions for the reheated configuration.

Parameter	Nominal Value
IHX cold-side outlet temp, °C	885
IHX effectiveness limit	<97%
IHX temperature pinch limit, °C	5
IHX LMTD, °C	15
Compressor outlet pressure, MPa	7.05
Precooler outlet temperature, °C	30
Recuperator effectiveness	95%
HTLHX effectiveness limit	<97%
HTLHX temperature pinch limit, °C	5
HTLHX LMTD, °C	27

D. Component Sizing and Pressure Drops

Once the cycle efficiencies had been calculated the relative size of the turbomachinery and heat exchangers was estimated. The actual size of the turbomachinery was not calculated but rather parameters that gave some indication to their relative size. HYSYS was used to calculate the energy output of the turbines as well as the energy needed for each compressor. The energy required for each component gives some indication of the size of the component. These relative energies were compared to determine the relative size of the turbomachinery.

To determine the relative sizes of the heat exchanger, the UA values (overall heat transfer coefficient time the heat transfer area) of the heat exchangers were calculated by HYSYS. The U values were calculated, the heat transfer areas were determined, and the heat exchanger volume was calculated. This gives a relative estimation of the heat exchanger sizes for the different configurations.

The IHX, HTLHX, and recuperator were assumed to be printed circuit heat exchangers as designed by Heatric[19]. PCHE are composed of channels chemically etched into plates. The plates are then stacked and diffusion bonded together and headers are attached to form the heat exchanger. For this study Alloy 617 was used as the construction material for the heat exchangers. The thermal conductivity was assumed to be constant over the length of the heat exchangers. The heat exchangers are assumed to be in counter flow to reduce the required surface area. The width and height of the heat exchangers were assumed to be equal. The flow channels are assumed to be semicircular with a diameter of 3 mm. From the stress analysis by Davis et al. the pitch to diameter ratio was taken as 1.2 and the plate thickness to diameter ratio was taken as .57 for the IHX, assuming a maximum hot side pressure of 7 MPa and a minimum cold side pressure of 5 MPa[2]. For the HTLHX and the recuperator the pitch to diameter ratio assumed as 1.7 and the plate thickness to diameter ratio was assumed as 1.19, assuming a maximum pressure of 7 MPa on one side and a minimum of 2 MPa on the other.

The overall heat transfer coefficient for was calculated as

$$U = \left(1/h_{hot} + 1/h_{cold} + t_{avg}/k_{metal} \right)^{-1}. \quad (9)$$

Where h_{hot} is the heat transfer coefficient for the hot channels, h_{cold} is the heat transfer coefficient for the cold channels, t_{avg} is the average thickness of the plates and k_{metal} is the thermal conductivity of the metal. The heat transfer coefficients were calculated using the Dittus-Boelter correlation[20],

$$Nu = 0.023\,\mathrm{Re}^{0.8}\,\mathrm{Pr}^{0.4} \quad (10)$$

where

$$Nu = h\frac{D_{hy}}{k}. \quad (11)$$

For laminar flow, the heat transfer coefficients were calculated from the exact solution for fully developed flow with constant heat rate[21],

$$Nu = 4.364. \quad (12)$$

The pressure drops in the heat exchangers were assumed to come from friction losses and were calculated using the following equation:

$$\Delta p = f\frac{L}{D_{hy}}\frac{G^2}{2\rho}, \quad (13)$$

where f is the friction factor, L is the length, D_{hy} is the hydraulic diameter of the channels, ρ is the density, and v is the velocity. The friction factor was determined using a correlation for turbulent and laminar flow. For turbulent flow f was calculated using

$$f = \frac{.3164}{\mathrm{Re}^{.25}}, \tag{14}$$

and for laminar flow

$$f = \frac{64}{\mathrm{Re}}. \tag{15}$$

A sizing algorithm for the heat exchangers was developed and entered into the spreadsheet function of HYSYS. The width, height, and pressure drops were assumed for the heat exchangers. Using the assumed channel diameter, pitch and thickness, the flow areas of the hot and cold streams were calculated. The values for ρ, μ, k, c_p and $\dot{m}$ for the inlet and outlet were obtained from HYSYS and averaged for the hot and cold side. The Reynolds number, Prandlt number, heat transfer coefficient and friction factor were then calculated for the hot and cold sides. The overall heat transfer coefficient was then calculated. The heat transfer area was then calculated by dividing the UA value given by HYSYS by the calculated heat transfer coefficient. The length of the heat exchanger is then calculated from the heat transfer area and the wetted perimeter of the channels. Using the length the pressure drops can then be calculated. For each heat exchanger one pressure drop was assumed to be constant. For the IHX the hot side pressure drop was assumed to be .05 MPa, for the HTLHX the cold side pressure drop was assumed to be .139 MPa, and for the recuperator the hot side pressure drop was assumed to be .100 MPa. Next the width and height were adjusted to match the set pressure drops in the heat exchangers. Finally the input values for the remaining pressure drops were adjusted to match the calculated pressure drops. Once the pressure drops converged the volume of the heat exchangers were calculated.

The steam generator was assumed to be a counter flow shell and tube heat exchanger. For the steam generator the Brayton cycle working fluid was on the shell side and the Rankine cycle on the tube side. Since the Brayton cycle working pressure, 7MPa, is lower than that for the Rankine cycle, 15 MPa, the pressure boundary requirements on the shell will be reduced[7,22]. Because the diameter of the tubes is small, normal tube thicknesses can endure the high pressure. A shell diameter of 4.5 m, an inner and outer diameter of 6 mm and 7.3 mm for the tubes, a pitch to outer diameter ratio of 1.3 and a triangular array were assumed for the steam generator. Again Alloy 617 was used for the construction material of the steam generator.

The overall heat transfer coefficient was calculated as[23],

$$U = \left(1/h_{cold} + d_{out}/2k_{metal} \ln\left(d_{out}/d_{in} \right) + d_{out}/d_{in}h_{hot} \right)^{-1}. \quad (16)$$

Where h_{hot} is the heat transfer coefficient for the hot channels, h_{cold} is the heat transfer coefficient for the cold channels, k_{metal} is the thermal conductivity of the metal and d_{in} and d_{out} are the inner and outer diameters of the tubes. The heat transfer coefficient on the hot side was calculated using Equation 10 for turbulent flow and for laminar flow Equation 12 was used.

To account for the phase change in the cold side, the steam generator was divided into four heat transfer regions: subcooled, nucleate boiling, post critical heat flux and superheated. On the hot side there is no phase change and Equations 10 and 12 were used to calculate the heat transfer coefficient and Equations 13-15 were used for the pressure drop calculations.

The subcooled region begins at the inlet to the steam generator and was assumed to end when the water reaches saturation conditions. Here we have neglected subcooled boiling. Since this region is single phase flow, Equations 10-15 were used for the heat transfer coefficient and pressure drop calculations.

The nucleate boiling region begins at the saturation point and ends when the fluid reaches critical quality. The Chen correlation was used in this region to determine the convection heat transfer coefficient. Chen assumes that the total convection coefficient in this region can be thought of as the superposition of the convection and nucleate boiling heat transfer coefficient[24],

$$h_{2\phi} = h_c + h_{NB} . \tag{17}$$

Chen assumed that the convective component, h_c, could be represented by a Dittus-Bolter type equation.

$$h_c = .023\left(\frac{G(1-x)D_{hy}}{\mu_f}\right)^{0.8}\left(\frac{\mu c_p}{k}\right)_f^{0.4}\left(\frac{k_f}{D_{hy}}\right)F , \tag{18}$$

where F is an additional correction factor defined as,

$$F = \left(\frac{\mathrm{Re}_{2\phi}}{\mathrm{Re}_f}\right)^{0.8} . \tag{19}$$

Chen originally determined F empirically; however he later derived F using a Reynolds analogy as follows,

$$F = \left(\phi_f^2\right)^{0.444} . \tag{20}$$

Here ϕ_f^2 is the two phase friction multiplier based on the pressure gradient from fluid alone. Using the Martinelli parameter ϕ_f^2 is defined as,

$$\phi_f^2 = 1 + \frac{C}{X} + \frac{1}{X^2}, \tag{21}$$

where C = 20 for turbulent-turbulent flow. The Martinelli parameter is based on the fluid properties at the saturation point and is defined as,

$$X = \left(\frac{1-x}{x}\right)^{0.9} \left(\frac{\rho_g}{\rho_f}\right)^{0.5} \left(\frac{\mu_f}{\mu_g}\right)^{0.1}. \tag{22}$$

The nucleate boiling component of the Chen correlation also uses fluid properties at the saturation point and is defined as,

$$h_{NB} = 0.00122 \left[\frac{\left(k^{0.79} c_p^{0.45} \rho^{0.49}\right)_f}{\sigma^{0.5} \mu_f^{0.29} h_{fg}^{0.24} \rho_g^{0.24}}\right] \Delta T_{sat}^{0.24} \Delta p_{sat}^{0.75} S, \tag{23}$$

where S is the suppression factor that takes into account the difference between the wall superheat and the mean superheat in the boundary layer. S can be calculated using[22],

$$S = \frac{1}{1 + 2.53 \times 10^{-6} \left(\mathrm{Re}_f \, F^{1.25}\right)^{1.17}}. \tag{24}$$

The Chen correlation determines the heat transfer coefficient at a point where the local quality is *x*. In this analysis a value of half the critical quality was chosen to give an average heat transfer coefficient over the entire region.

To determine the length and volume of the nucleate boiling region of the heat exchanger, the critical quality must be known. In order to determine the critical quality an iterative process must be implemented. First an initial guess of the critical quality must be made; in this case .75 was used. Using this initial guess the tube side heat

transfer coefficient is determined along with the universal heat transfer coefficient. Using the ε-NTU method, the heat transfer area is determined. The effectiveness of the heat exchanger in this region was calculated using Equation 2. The NTU value was calculated using,

$$NTU = \frac{1}{C_r - 1}\ln\left(\frac{\varepsilon - 1}{\varepsilon C_r - 1}\right) \qquad C_r < 1 \tag{25}$$

$$NTU = \frac{\varepsilon}{1-\varepsilon} \qquad C_r = 1 \tag{26}$$

where $C_r = C_{min/}\, C_{max}$.

Next the heat transfer area and the length were calculated,

$$A = \frac{NTU}{U} C_{\min} \tag{27}$$

$$l = \frac{A}{\pi d_{in} N_t} \tag{28}$$

where d_{in} is the inside diameter of the tubes and N_t is the number of tubes in the heat exchanger. The number of tubes is given by the follow formula,

$$N_t = \frac{d_{in,shell}^2 \pi}{4 p^2 \sin\left(\pi/3\right)}. \tag{29}$$

where $d_{in,shell}$ is the inner diameter of the shell and p is the pitch. The length is then inserted into the CISE-4 correlation and a new critical quality is calculated and reiterated until it converges. The CISE-4 correlation is given by[25],

$$x_{crit} = \frac{a_{CISE4} l_{crit}}{l_{crit} + b_{CISE4}} \tag{30}$$

$$a_{CISE4} = \frac{1}{1 + 1.481 \times 10^{-4} \left(1 - \frac{p}{p_c}\right)^{-3} G} \qquad G < G^* \tag{31}$$

$$a_{CISE4} = \frac{1 - \frac{p}{p_c}}{\left(\frac{G}{1000}\right)^{1/3}} \qquad G < G^* \tag{32}$$

$$b_{CISE4} = 0.199 \left(\frac{p_c}{p} - 1\right)^{0.4} G * d_{in,tube}^{0.4} \tag{33}$$

$$G^* = 3375 \left(1 - \frac{p_c}{p}\right)^3 \tag{34}$$

where p_c is the critical pressure of water. The pressure drop calculation was performed by multiply the pressure drop calculated assuming the total fluid as liquid, Δp_{fo}, and multiplying by a two phase friction multiplier, ϕ_{fo}^2.

$$\Delta p = \Delta p_{fo} \phi_{fo}^2 \tag{35}$$

$$\Delta p = f_{fo} \frac{L}{D_{hy}} \frac{G^2}{2\rho_f} \tag{36}$$

Collier and Thome recommend the Friedel correlation for the two phase friction multiplier for flows where[24],

$\mu_f / \mu_g < 1000$.

The Friedel correlation is given in Collier and Thome as[24],

$$\phi_{fo}^2 = A_1 + \frac{3.24 A_2 A_3}{Fr^{0.045} We^{0.035}} \tag{37}$$

where

$$A_1 = (1-x)^2 + x^2 \left(\frac{\rho_f f_{go}}{\rho_g f_{fo}} \right) \tag{38}$$

$$A_2 = x^{0.78} (1-x)^{0.224} \tag{39}$$

$$A_3 = \left(\frac{\rho_f}{\rho_g} \right)^{0.91} \left(\frac{\mu_g}{\mu_f} \right)^{0.19} \left(1 - \frac{\mu_g}{\mu_f} \right)^{.7} \tag{40}$$

$$Fr = \frac{G^2}{gD\overline{\rho}^2} \tag{41}$$

$$We = \frac{G^2 D}{\overline{\rho}\sigma} \tag{42}$$

In the post critical heat flux region which ranges from dry-out to the end of saturation, the Groeneveld correlation was used. This is a common method used in calculating the heat transfer in the region and is given by the following equation[22],

$$Nu = 0.00109\left\{\mathrm{Re}_g\left[x+\frac{\rho_g}{\rho_f}(1-x)\right]\right\}^{0.989}\mathrm{Pr}_g^{1.41}\,Y \tag{43}$$

$$Y = \left[1-0.1\left(\frac{\rho_f-\rho_g}{\rho_g}\right)^{0.4}(1-x)^{0.4}\right]^{-1.15}. \tag{44}$$

Again an average quality is used to give an average heat transfer coefficient over the region. The pressure drop calculation in the region was performed using the Friedel correlation that was used in the nucleate boiling region.

For the superheat region the heat transfer becomes single phase and Equations 10-15 were used to calculate the heat transfer coefficient and the pressure drop. Average properties were used to calculate the heat transfer coefficient and the pressure drop. Since this design assumes ad superheat of 575 °C, this region accounts for the majority of the heat exchanger volume.

A similar algorithm as before was used in the steam generator sizing. Using the assumed shell diameter, tube inner and outer diameter, pitch, triangular array and pressure drops the overall heat transfer coefficient and heat transfer area were found for each heat transfer region. The length of each region was then obtained from the heat transfer area and the shell diameter. The hot and cold side pressure drops were then calculated. The pressure drop was then iterated until the input and output values converged. Once all the regions were solved the total volume and pressure drop in the steam generator was calculated by summing the volume and pressure drops from each region.

E. Parametric Studies

Parametric studies away from the baseline values of the systems were performed on the three-shaft and combined cycles to determine the effect of varying conditions in the cycle. This gives insight into the sensitivity of these cycles to various operating. The parametric studies were carried out by isolating and varying a single working condition. Once the working condition was changed the cycle was optimized using the methods discussed in Section III.C.

The reactor outlet temperature for the NGNP is limited by material concerns. Past designs such as the Arbeitsgemeinschaft Versuchsreactok (AVR) have been operating at reactor outlet temperatures of 950°C. The Chinese HTR-10 was design to operate up to 950°C to investigate diverse power generation systems (e.g. gas turbine) and nuclear process heat applications. With current materials reactor outlet temperatures up to 1000°C can be realized but with a limited lifetime of 15 to 20 years[26]. Reactor outlet temperature was studied to determine the efficiency increase gained by using these higher temperatures. The reactor outlet temperature was varied from 900°C to 1000°C. At each reactor outlet temperature the cycles were optimized. Assuming that at each temperature the plant design would be optimized the heat exchangers were resized; however, in the case the reactor outlet temperature was raised after the plant had been constructed the heat exchangers would not be resized.

The sensitivity of the cycle to mass flow was studied to determine the effects of loss of coolant on the system. The mass flow was varied between 85-100% and the cycles were optimized at the lower flow rates. Since this study is for off nominal behavior of the optimized cycles the heat exchangers were not resized.

The pressure in the secondary side was studied to establish the effects running the cycle at a lower pressure. The pressure was varied between 2 MPa and 7 MPa and the cycles were optimized at each pressure. The heat exchangers were resized to give the optimal plant design.

In high temperature systems turbine cooling may be needed prolong the life of the turbines. This is done by splitting the outlet flow of the high temperature compressor. Most of the flow continues through the cycle while a fraction goes towards cooling the turbines. The split flow then cools the turbines and returns to the main flow inside the turbine[27].

A simplified model of turbine cooling was used to model the process. A single-stage turbine with cooling of the disc, stator blades and rotor blades was assumed. The mass flow to the stator blade and disc cooling add to the work in the turbine while the rotor cooling does not [27]. It was assumed that since the cooling mass flow was small, the reduction in temperature of the working fluid due to cooling is neglected. Therefore, since the mass flow of the stator blade and disc cooling add to the work and their temperature difference is neglected they can be ignored in the calculation of the turbine work. The rotor cooling can be modeled as a loss of flow through the turbine. The model splits the outlet flow from the high pressure compressor with a small fraction going towards the turbine cooling and the rest continues through the cycle. It was assumed that 4% of the flow was need for the high temperature turbine and 2% was need for each additional turbine. This gives 4% for cooling in the combined cycle and 8% for cooling in the three-shaft cycle. Turbine cooling was applied to the configurations, the cycles were optimized and the heat exchangers were resized.

III. RESULTS*

The methods described in Section III were applied to the three configurations as stated in the section. The PCU efficiency was calculated for each configuration. Sections IV.A through IV.C present the results for the three-shaft, combined and reheated cycles. The effects of the ITHL working fluid and the HTSE plant on total plant efficiency are presented in Section IV.D.

A. Three-Shaft Design

The three-shaft configuration illustrated in Figure 4 is an indirect cycle with a three-shaft PCU configuration and an intermediate heat transport loop for hydrogen production. The primary side of the loop consists of a high temperature nuclear reactor, IHX, and a circulator. The conditions for this loop are summarized in Table I. The PCU configuration, illustrated in Figure 4, consists of; (1) a primary loop (2) an intermediate heat transport loop in parallel with (3) the PCU with three turbines (high pressure turbine, low pressure turbine and power turbine), 4 compressors (low pressure compressor, medium pressure compressor 1, medium pressure compressor 2, and high pressure compressor) 1 precooler, 3 intercoolers and a recuperator. Helium, CO_2 and the N_2-He mixture were simulated in the PCU and the results are described in Sections 1, 2 and 3, respectively. Section 4 describes the results from the parametric studies.

Comparing the working fluids in this cycle it can be seen that the helium working fluid produces the highest efficiency. However, it also has large heat exchangers and turbomachinery. Using the N_2-He mixture produces a slightly lower efficiency but with smaller heat exchangers. The CO_2 working fluid has a much lower, approximately 4%, cycle efficiency than the helium and N_2-He mixture. CO_2 does have the largest heat

* Part of this section is reprinted with permission from "Evaluation of Working Fluids in an Indirect Combined Cycle in a Very High Temperature Gas-Cooled Reactor" by Chang Oh, Robert Barner, Cliff Davis and Steve Sherman, 2006. *Nuclear Technology*, 156, 1-10. Copyright 2006 by American Nuclear Society, La Grange Park, IL.

exchanger size, however, the turbomachinery is smaller that that of the helium and N_2-He mixture.

1. Helium Working Fluid

The helium working fluid was optimized for the three-shaft cycle with a pressure ratio of 3.432 and a PCU efficiency of 50.93%. The secondary mass flow rate was optimized at 289 kg/s. The HYSYS simulation is illustrated in Figure 8, the T-S diagram is shown in Figure 9 and the state points are summarized in Table VII. The total heat exchanger volume was 242.5 m^3 and the total cycle work was 800.2 MW. Table VIII lists the individual component sizing results for the cycle.

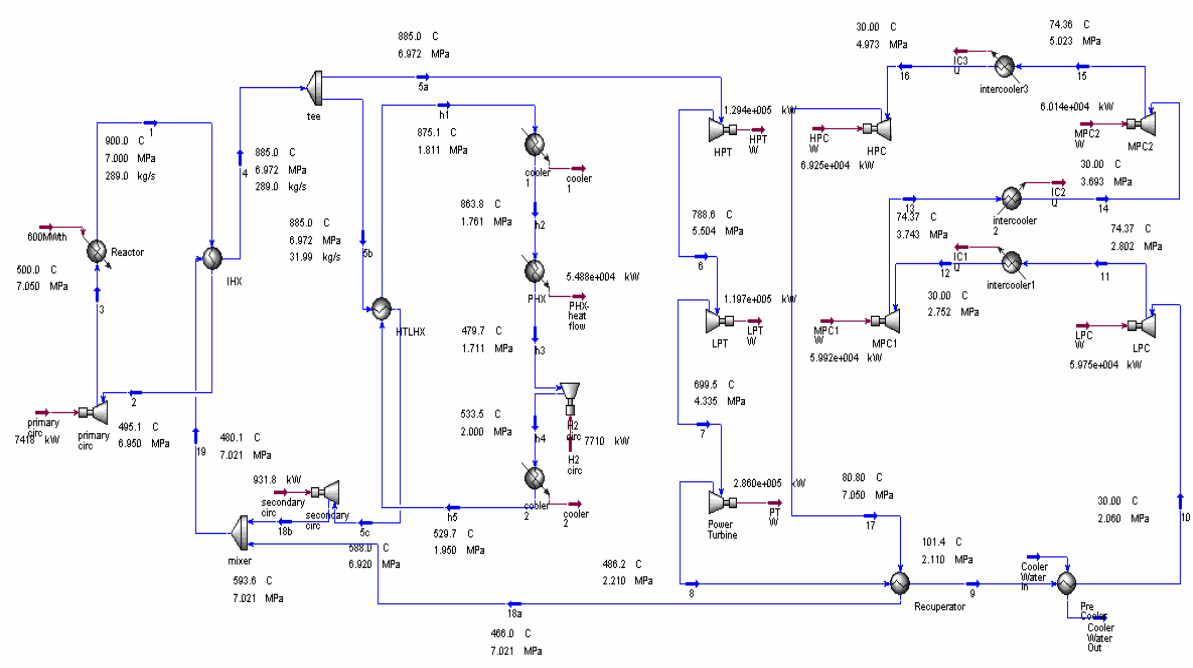

Figure 8. HYSYS diagram of three-shaft configuration with helium working fluid.

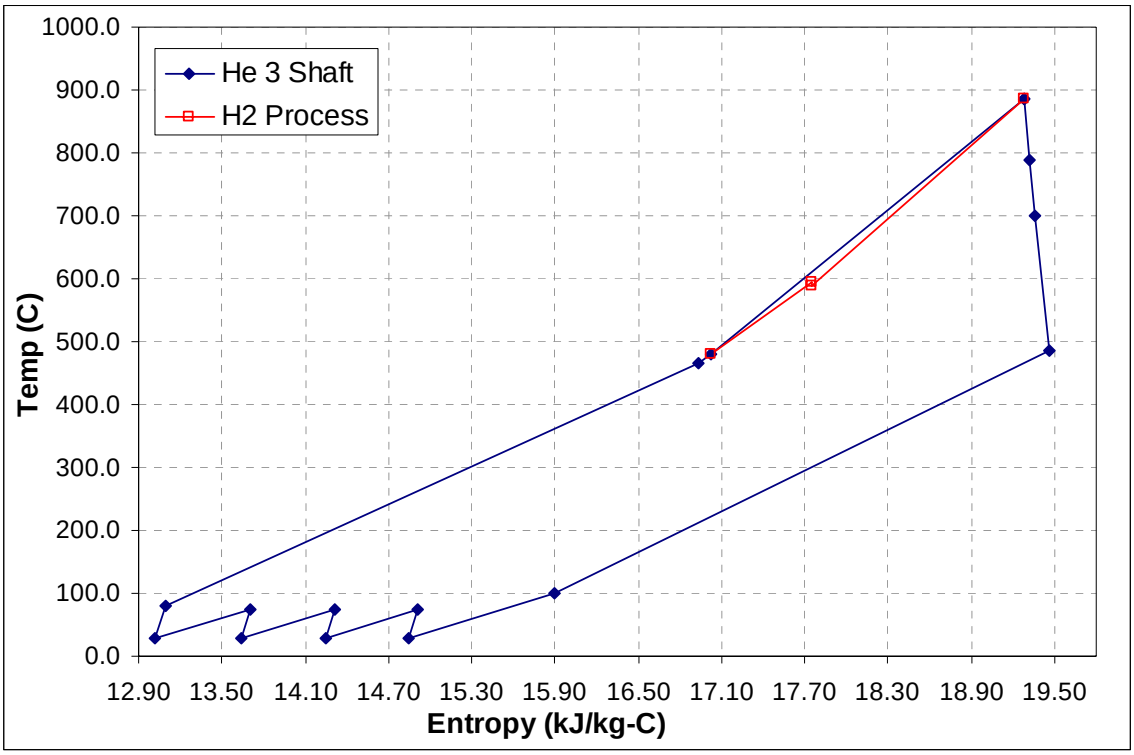

Figure 9. T-S diagram for three-shaft configuration with helium working fluid.

TABLE VII
State points for three-shaft configuration with helium working fluid.

Point	Temp (°C)	Pressure (Mpa)	Entropy (kJ/kg-K)	Enthalpy (kJ/kg)
1	900.0	7.00	19.33	4561.1
2	495.1	6.95	17.15	2459.0
3	500.0	7.05	17.16	2484.7
4,5(a,b)	885.0	6.97	19.28	4483.2
5c	588.0	6.92	17.75	2941.3
6	788.6	5.50	19.32	3979.7
7	699.5	4.33	19.36	3514.0
8	486.2	2.21	19.47	2401.3
9	101.4	2.11	15.89	402.6
10	30.0	2.06	14.84	31.7
11	74.4	2.80	14.92	264.2
12	30.0	2.75	14.24	33.7
13	74.4	3.74	14.32	266.8
14	30.0	3.69	13.63	36.3
15	74.4	5.02	13.71	270.3
16	30.0	4.97	13.02	39.8
17	80.8	7.05	13.10	309.3
18a	466.0	7.02	16.93	2307.9
18b	593.6	7.02	17.76	2970.4
19	480.1	7.02	17.03	2381.3

TABLE VIII
Component sizing data for three-shaft configuration with helium working fluid.

Component	Value
Turbine work (MW)	535.0
Compressor work (MW)	249.1
Circulator work (MW)	8.4
IHX volume (m^3)	80.5
HTLHX volume (m^3)	9.1
Recuperator volume (m^3)	153

2. CO_2 Working Fluid

The CO_2 working fluid was optimized for the three-shaft cycle with a pressure ratio of 22.57 and a PCU efficiency of 46.73%. The secondary mass flow rate was optimized at 1201 kg/s. The HYSYS simulation is illustrated in Figure 10, the T-S diagram is shown in Figure 11 and the state points are summarized in Table IX. The total heat exchanger volume was 285.2 m^3 and the total cycle work was 729.8 MW. Table X lists the individual component sizing results for the cycle.

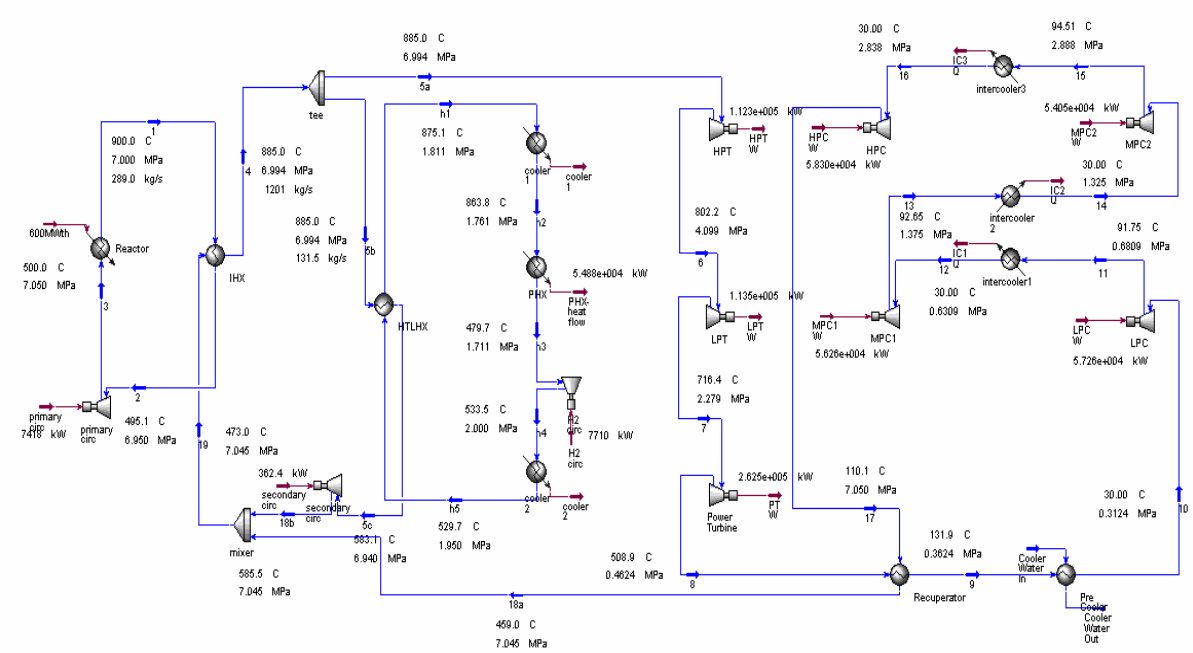

Figure 10. HYSYS diagram of three-shaft configuration with CO_2 working fluid.

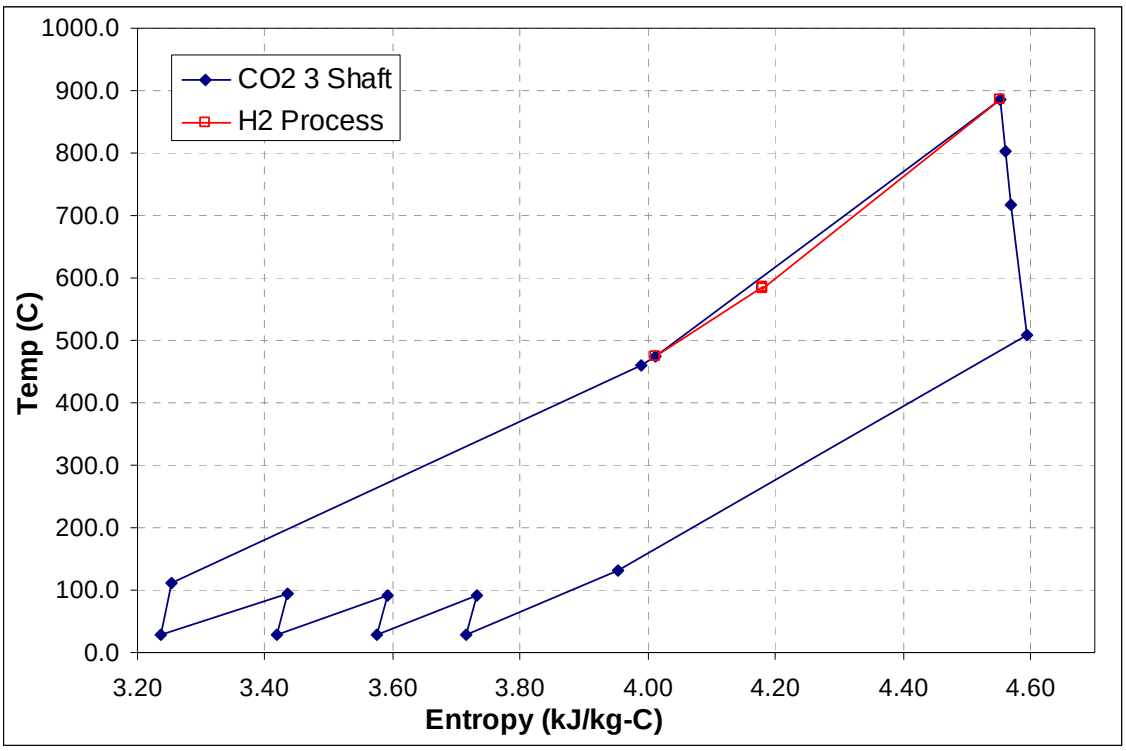

Figure 11. T-S diagram of three-shaft configuration with CO_2 working fluid.

TABLE IX
State points for three-shaft configuration with CO2 working fluid.

Point	Temp (°C)	Pressure (Mpa)	Entropy (kJ/kg-K)	Enthalpy (kJ/kg)
1	900.0	7.00	19.33	4561.1
2	495.1	6.95	17.15	2459.0
3	500.0	7.05	17.16	2484.7
4,5(a,b)	885.0	6.99	4.55	-7999.0
5c	583.1	6.94	4.18	-8374.2
6	802.2	4.10	4.56	-8104.0
7	716.4	2.28	4.57	-8210.1
8	508.9	0.46	4.59	-8455.5
9	131.9	0.36	3.95	-8852.9
10	30.0	0.31	3.71	-8946.3
11	91.7	0.68	3.73	-8892.8
12	30.0	0.63	3.57	-8949.4
13	92.6	1.38	3.59	-8896.8
14	30.0	1.33	3.42	-8956.2
15	94.5	2.89	3.43	-8905.7
16	30.0	2.84	3.24	-8972.8
17	110.1	7.05	3.25	-8918.3
18a	459.0	7.05	3.99	-8521.0
18b	585.5	7.05	4.18	-8371.5
19	473.0	7.05	4.01	-8504.6

TABLE X
Component sizing data for three-shaft configuration with CO_2 working fluid.

Component	Value
Turbine work (MW)	488.4
Compressor work (MW)	225.9
Circulator work (MW)	8.1
IHX volume (m^3)	107.3
HTLHX volume (m^3)	11.5
Recuperator volume (m^3)	166.3

3. Nitrogen-Helium Working Fluid

The N_2-He mixture was optimized for the three-shaft cycle with a pressure ratio of 4.436 and a PCU efficiency of 50.76%. The secondary mass flow rate was optimized at 759 kg/s. The HYSYS simulation is illustrated in Figure 12, the T-S diagram is shown in Figure 13 and the state points are summarized in Table XI. The total heat exchanger volume was 227.7 m^3 and the total cycle work was 799.4 MW. Table XII lists the individual component sizing results for the cycle.

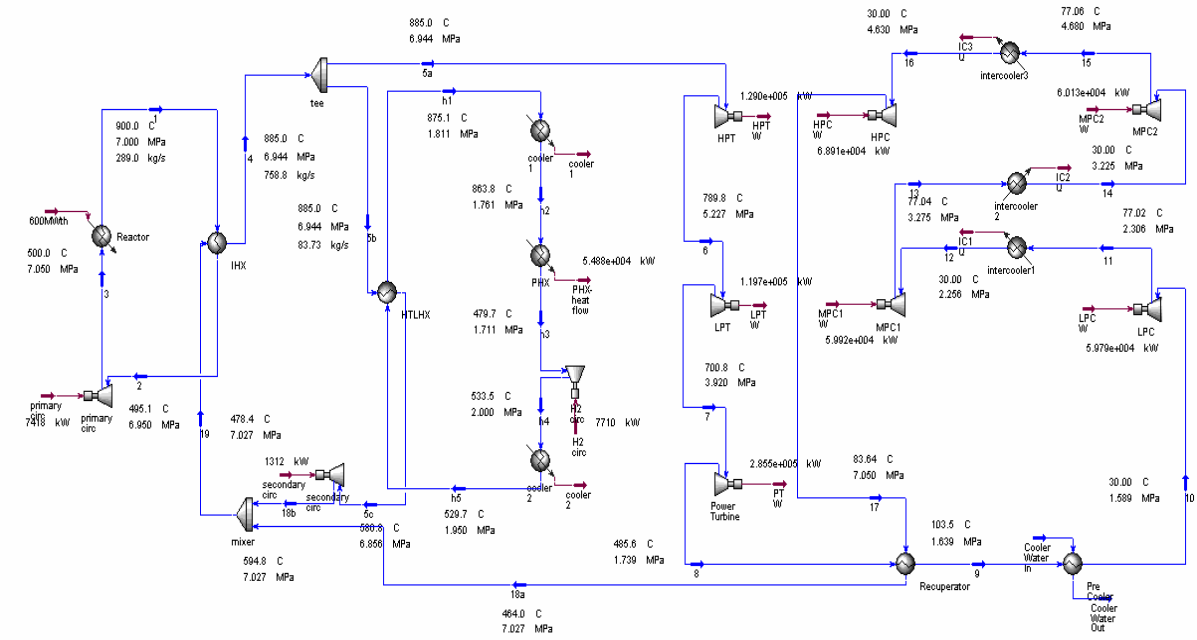

Figure 12. HYSYS diagram of three-shaft configuration with a nitrogen-helium mixture working fluid.

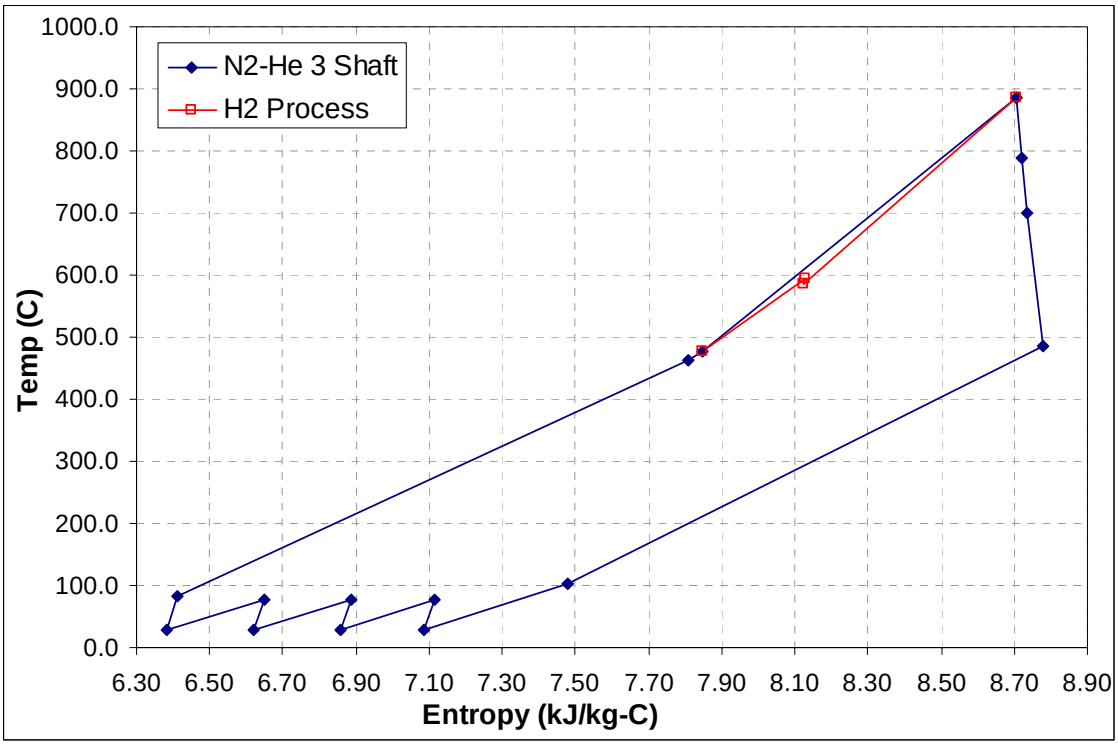

Figure 13. T-S diagram of three-shaft configuration with a nitrogen-helium mixture working fluid.

TABLE XI
State points for three-shaft configuration with a nitrogen-helium mixture working fluid.

Point	Temp (°C)	Pressure (Mpa)	Entropy (kJ/kg-K)	Enthalpy (kJ/kg)
1	900.0	7.00	19.33	4561.1
2	495.1	6.95	17.15	2459.0
3	500.0	7.05	17.16	2484.7
4,5(a,b)	885.0	6.94	8.71	1670.4
5c	586.8	6.86	8.13	1081.3
6	789.8	5.23	8.72	1479.2
7	700.8	3.92	8.74	1301.9
8	485.6	1.74	8.78	879.0
9	103.5	1.64	7.48	147.5
10	30.0	1.59	7.09	8.8
11	77.0	2.31	7.12	97.4
12	30.0	2.26	6.86	8.6
13	77.0	3.27	6.88	97.4
14	30.0	3.22	6.62	8.4
15	77.1	4.68	6.65	97.4
16	30.0	4.63	6.38	8.1
17	83.6	7.05	6.41	110.2
18a	464.0	7.03	7.81	841.7
18b	594.8	7.03	8.13	1096.9
19	478.4	7.03	7.85	869.9

TABLE XII
Component sizing data for three-shaft configuration with a nitrogen-helium mixture working fluid.

Component	Value
Turbine work (MW)	534.2
Compressor work (MW)	248.7
Circulator work (MW)	8.7
IHX volume (m^3)	71.4
HTLHX volume (m^3)	8.2
Recuperator volume (m^3)	148.2

4. Parametric Studies

Parametric studies were performed on the reactor outlet temperature, secondary mass flow rate, pressure, and turbine for the 3 working fluids. The results are summarized in Figure 14, Figure 15, Figure 16 and Table XIII. Helium and the N_2-He mixture behaved similarly under off normal working conditions. It can be noted from Figure 14 that at a reactor outlet temperature of 1000 °C the efficiency of the nitrogen-helium mixture surpasses that of the helium. The off normal conditions had a greater influence on the CO_2 than the other two fluids. The effect of turbine cooling on the system was an approximately 3% efficiency decrease for all working fluids.

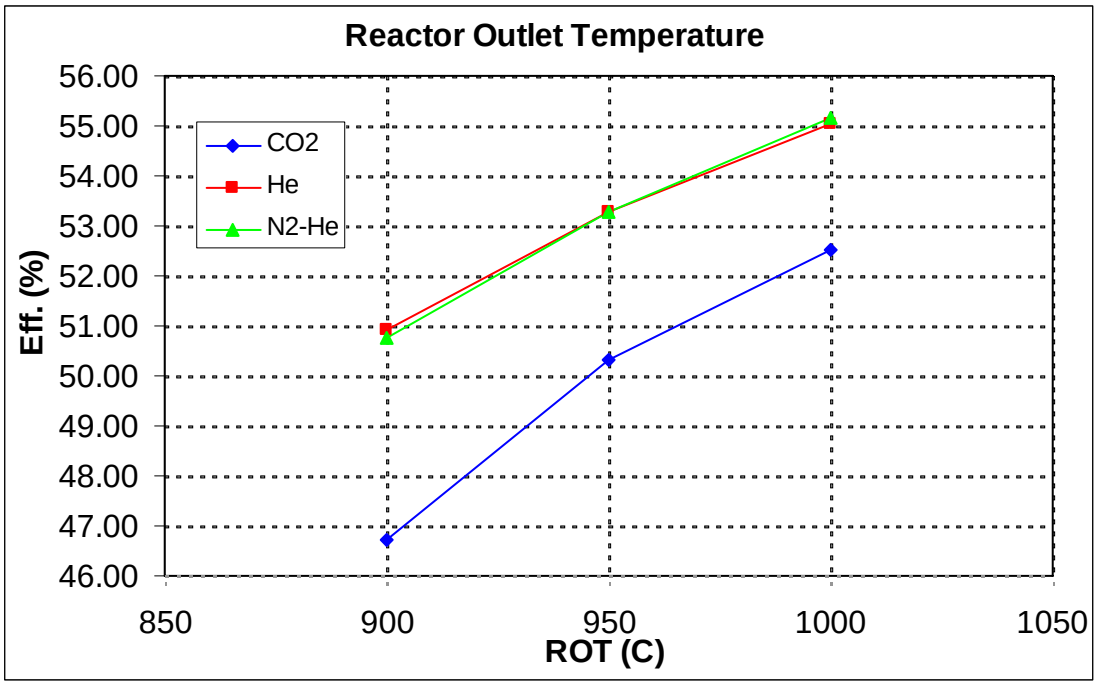

Figure 14. Parametric study of the effects of reactor outlet temperature on three- shaft cycle efficiency.

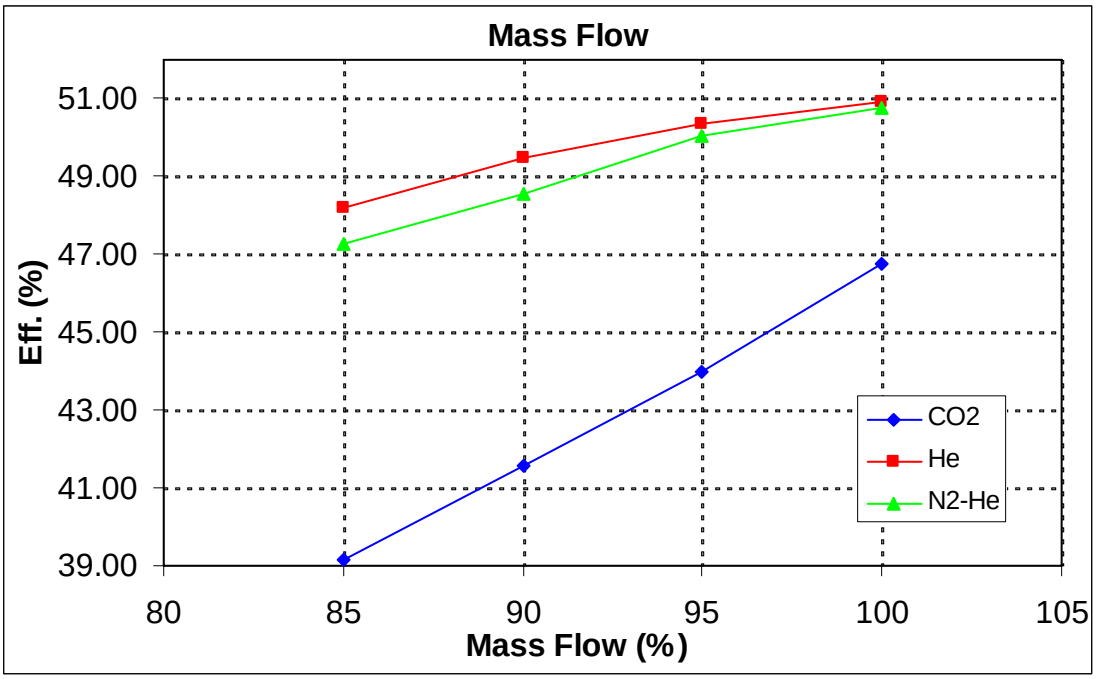

Figure 15. Parametric study of the effects of secondary mass flow rate on three- shaft cycle efficiency.

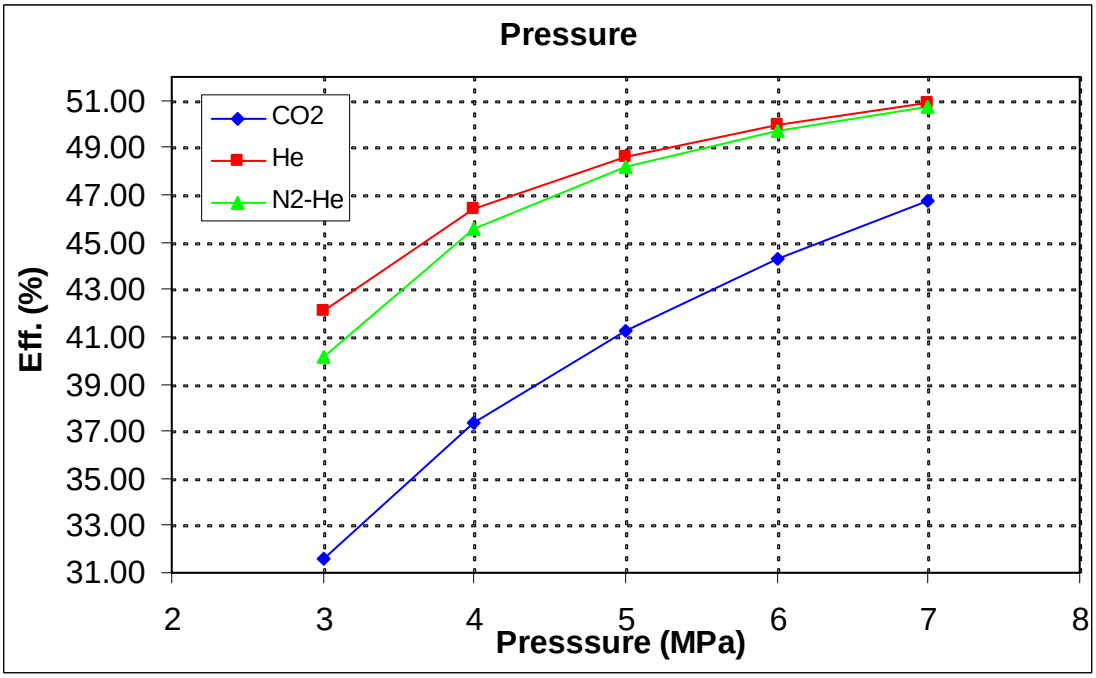

Figure 16. Parametric study of the effects of working pressure on three- shaft cycle efficiency.

TABLE XIII
Parametric study of the effects of turbine cooling on three- shaft cycle efficiency.

Turbine Cooling			
	CO2	**He**	**N2-He**
None	46.73	50.93	50.76
8%	43.14	47.75	47.06

B. Combined Cycle

The combined cycle is an indirect cycle with a combined PCU configuration and an intermediate heat transport loop for hydrogen production. The PCU configuration, illustrated in Figure 5, consists of; (1) a primary loop (2) an intermediate heat transport loop in parallel with (3) the PCU with a Brayton top cycle consisting of a gas turbine, compressor and coupled to a Rankine bottoming cycle through a steam generator. The Rankine cycle consists of a steam turbine, condenser and a pump. This cycle was simulated using helium as the working fluid in the primary and intermediate heat transport loop. Helium, CO_2 and the N_2-He mixture were simulated in the PCU and the results are described in Sections 1, 2 and 3, respectively. Section 4 describes the results from the parametric studies.

The same Rankine bottoming cycle was used for all three working fluids. This cycle gets heat from the Brayton cycle through a steam generator located between the gas turbine and compressor. The steam turbine inlet temperature was set at 575°C to take advantage of the superheat option and keep the turbine outlet quality at 85%. A T-S diagram of the cycle is illustrated in Figure 17 and the state points are summarized in TABLE XIV.

Comparing the working fluids in this cycle it can be seen that the CO_2 working fluid produces the highest efficiency and smallest component sizes. Helium and the N_2-He mixture produced similar component sizes; however, helium had a slightly higher efficiency.

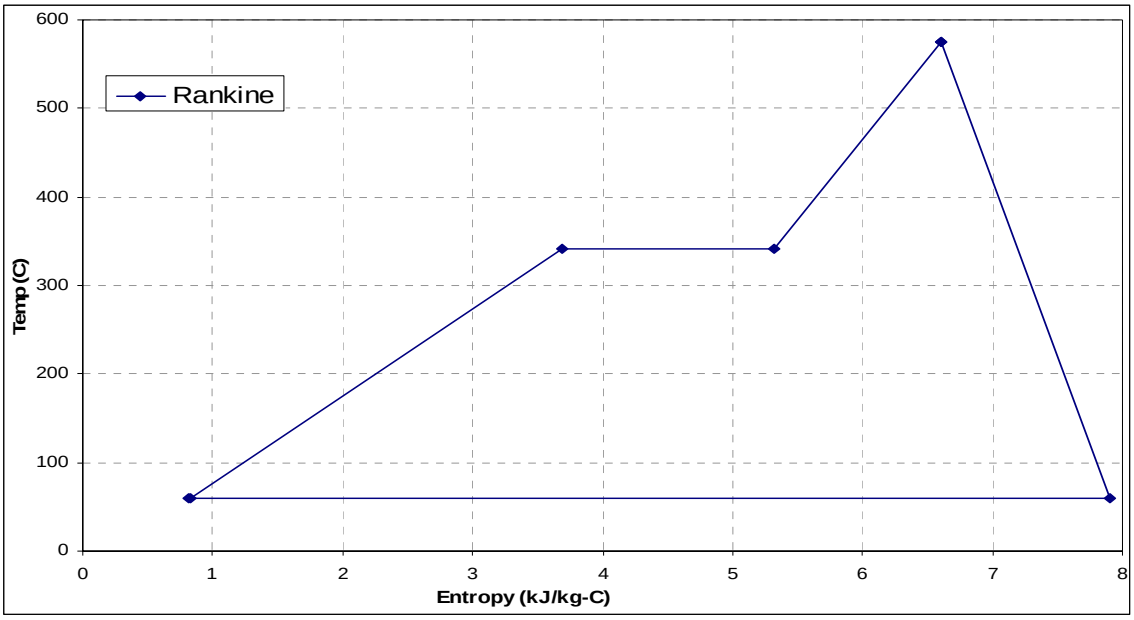

Figure 17. T-S diagram for Rankine bottoming cycle.

TABLE XIV
State points for Rankine bottoming cycle.

Point	Temp (°C)	Pressure (Mpa)	Entropy (kJ/kg-K)	Enthalpy (kJ/kg)
S1	575.0	15.00	6.6	-12428.8
S2	60.2	0.02	7.9	-13671.8
S3	59.0	0.02	0.82	-15695.9
S4	59.8	15.00	0.83	-15678.9

1. Helium Working Fluid

The helium working fluid was optimized for the combined cycle with a pressure ratio of 2.281 and an efficiency of 49.10%. The secondary mass flow rate was optimized at 289 kg/s. The HYSYS simulation is illustrated in Figure 18, the T-S diagram is shown in Figure 19 and the state points are summarized in Table XV. The total heat exchanger volume was 216.0 m^3 and the total cycle work was 700.1 MW. Table XVI lists the individual component sizing results for the cycle.

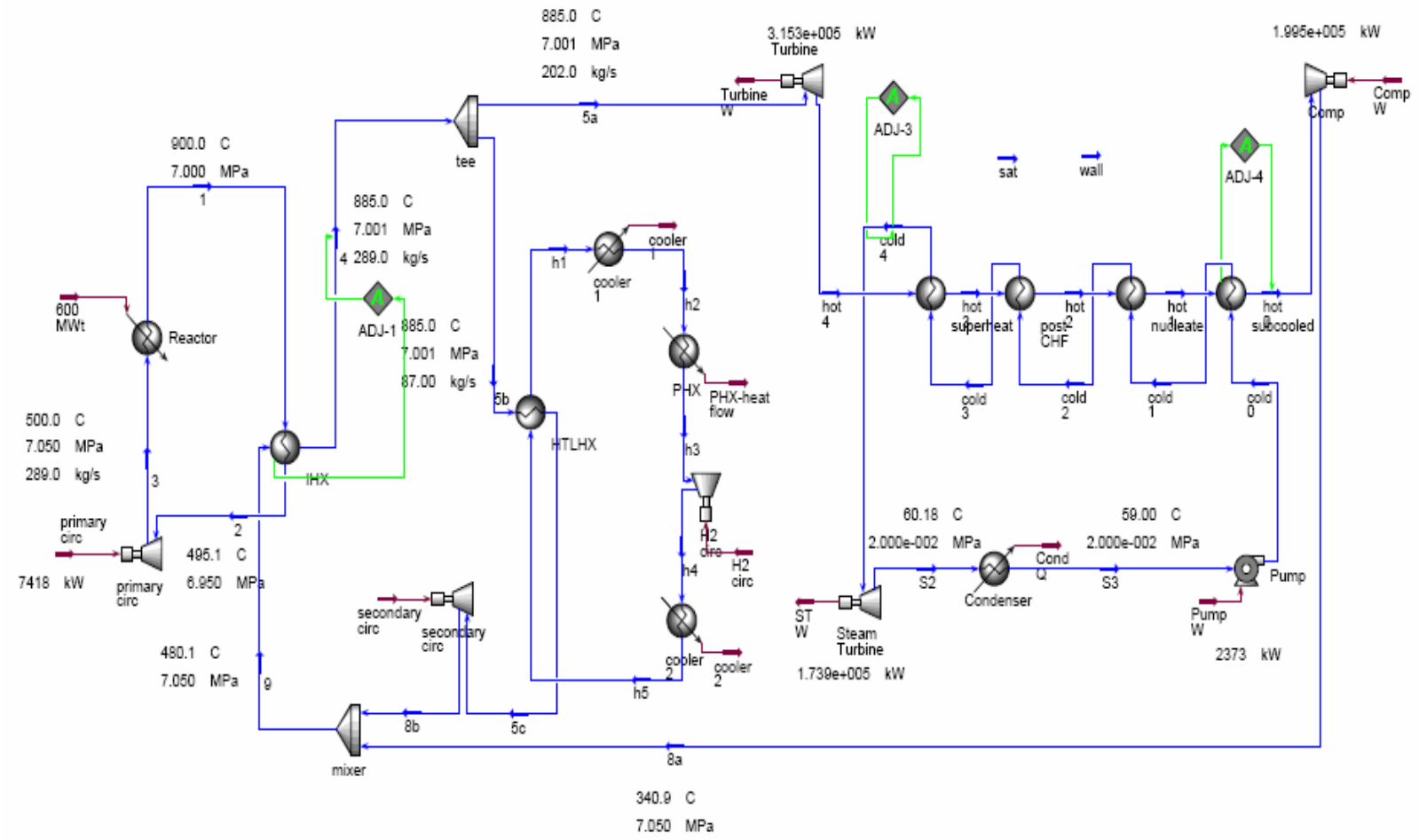

Figure 18. HYSYS diagram of the combined cycle with helium working fluid.

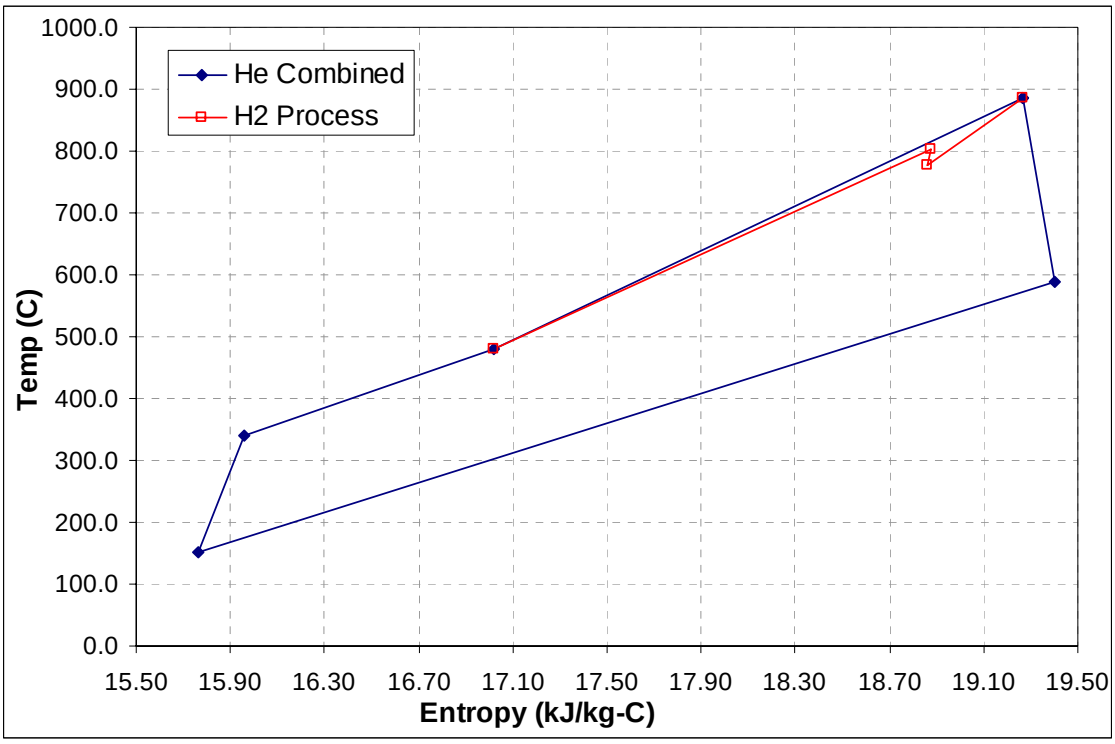

Figure 19. T-S diagram for combined cycle with helium working fluid.

TABLE XV
State points for Brayton top cycle with helium working fluid.

Point	Temp (°C)	Pressure (Mpa)	Entropy (kJ/kg-K)	Enthalpy (kJ/kg)
1	900.0	7.00	19.33	4561.1
2	495.1	6.95	17.15	2459.0
3	500.0	7.05	17.16	2484.7
4,5(a,b)	885.0	7.00	19.27	4483.2
5c	775.9	6.65	18.86	3916.3
6	587.5	3.12	19.40	2929.8
7	151.5	3.07	15.77	665.4
8a	340.9	7.05	15.96	1658.8
8b	803.1	7.05	18.87	4058.3
9	480.1	7.05	17.02	2381.2

TABLE XVI
Component sizing data for combined cycle with helium working fluid.

Component	Value
Gas Turbine work (MW)	315.3
Steam Turbine work (MW)	173.9
Compressor work (MW)	201.8
Pump work (MW)	2.4
Circulator work (MW)	9.4
IHX volume (m^3)	80.4
HTLHX volume (m^3)	1.7
Steam generator volume (m^3)	133.9

2. CO_2 Working Fluid

The CO_2 working fluid was optimized for the combined cycle with a pressure ratio of 7.62 and a PCU efficiency of 50.50%. The secondary mass flow rate was optimized at 1113 kg/s. The HYSYS simulation is illustrated in
Figure 20, the T-S diagram is shown in Figure 21 and the state points are summarized in XVII. The total heat exchanger volume was 218.6 m^3 and the total cycle work was 655.1 MW. Table XVIII lists the individual component sizing results for the cycle.

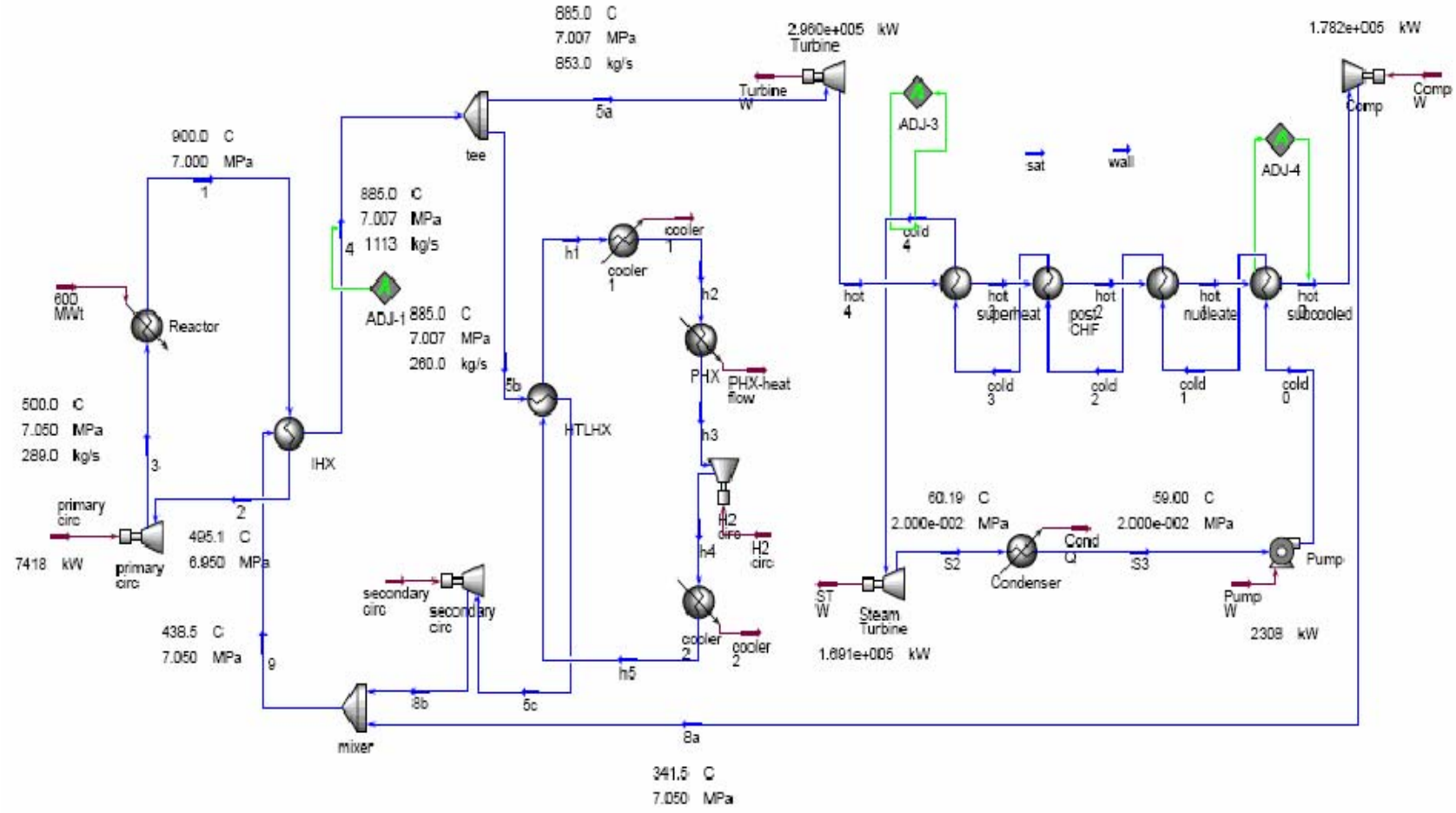

Figure 20. HYSYS diagram of Brayton top cycle with CO_2 working fluid.

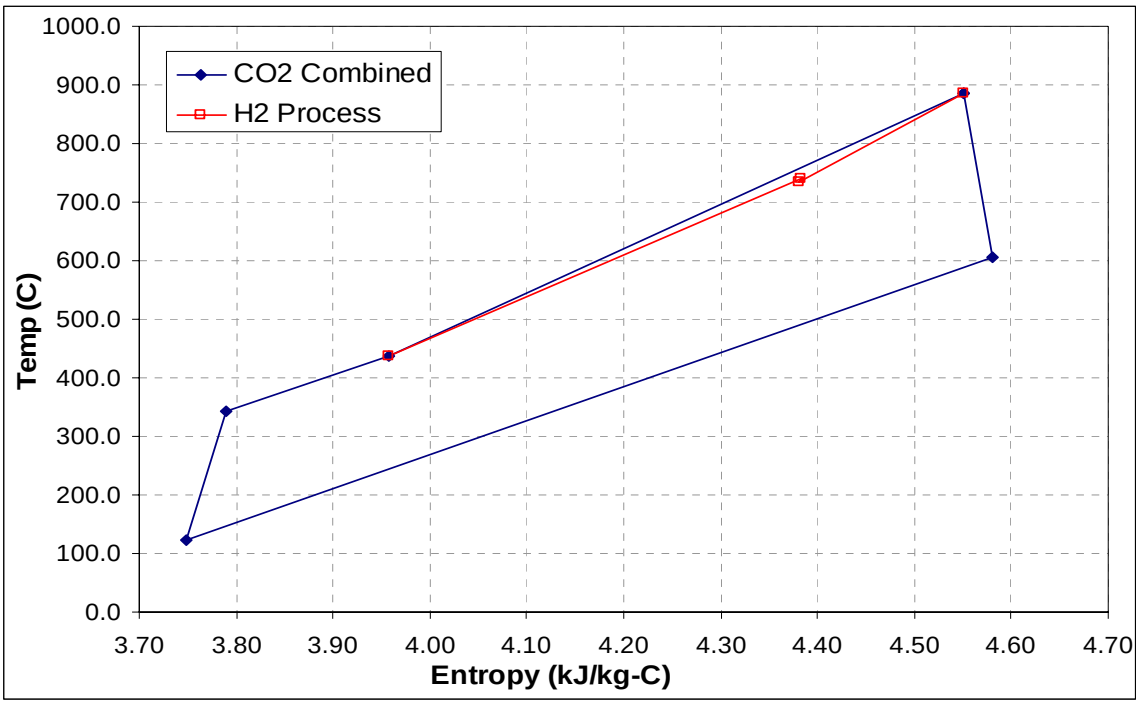

Figure 21. T-S diagram of Brayton top cycle with CO_2 working fluid.

TABLE XVII
State points for Brayton top cycle with CO_2 working fluid.

Point	Temp (°C)	Pressure (Mpa)	Entropy (kJ/kg-K)	Enthalpy (kJ/kg)
1	900.0	7.00	19.33	4561.1
2	495.1	6.95	17.15	2459.0
3	500.0	7.05	17.16	2484.7
4,5(a,b)	885.0	7.01	4.55	-7999.0
5c	734.8	6.81	4.38	-8188.7
6	609.0	1.04	4.58	-8339.2
7	118.8	0.88	3.75	-8868.4
8a	341.6	7.05	3.79	-8655.5
8b	741.0	7.05	4.38	-8181.1
9	438.5	7.05	3.96	-8544.7

TABLE XVIII
Component sizing data for combined cycle with CO_2 working fluid.

Component	Value
Gas Turbine work (MW)	296.0
Steam Turbine work (MW)	169.1
Compressor work (MW)	178.2
Pump work (MW)	2.3
Circulator work (MW)	9.4
IHX volume (m^3)	48.5
HTLHX volume (m^3)	2.6
Steam generator volume (m^3)	167.5

3. Nitrogen-Helium Working Fluid

The N_2-He mixture was optimized for the combined cycle with a pressure ratio of 2.68 and an efficiency of 48.70%. The secondary mass flow rate was optimized at 759 kg/s. The HYSYS simulation is illustrated in Figure 22, the T-S diagram is shown in Figure 23 and the state points are summarized in Table XIX. The total heat exchanger volume was 203.8 m^3 and the total cycle work was 719.1 MW. Table XX lists the individual component sizing results for the cycle.

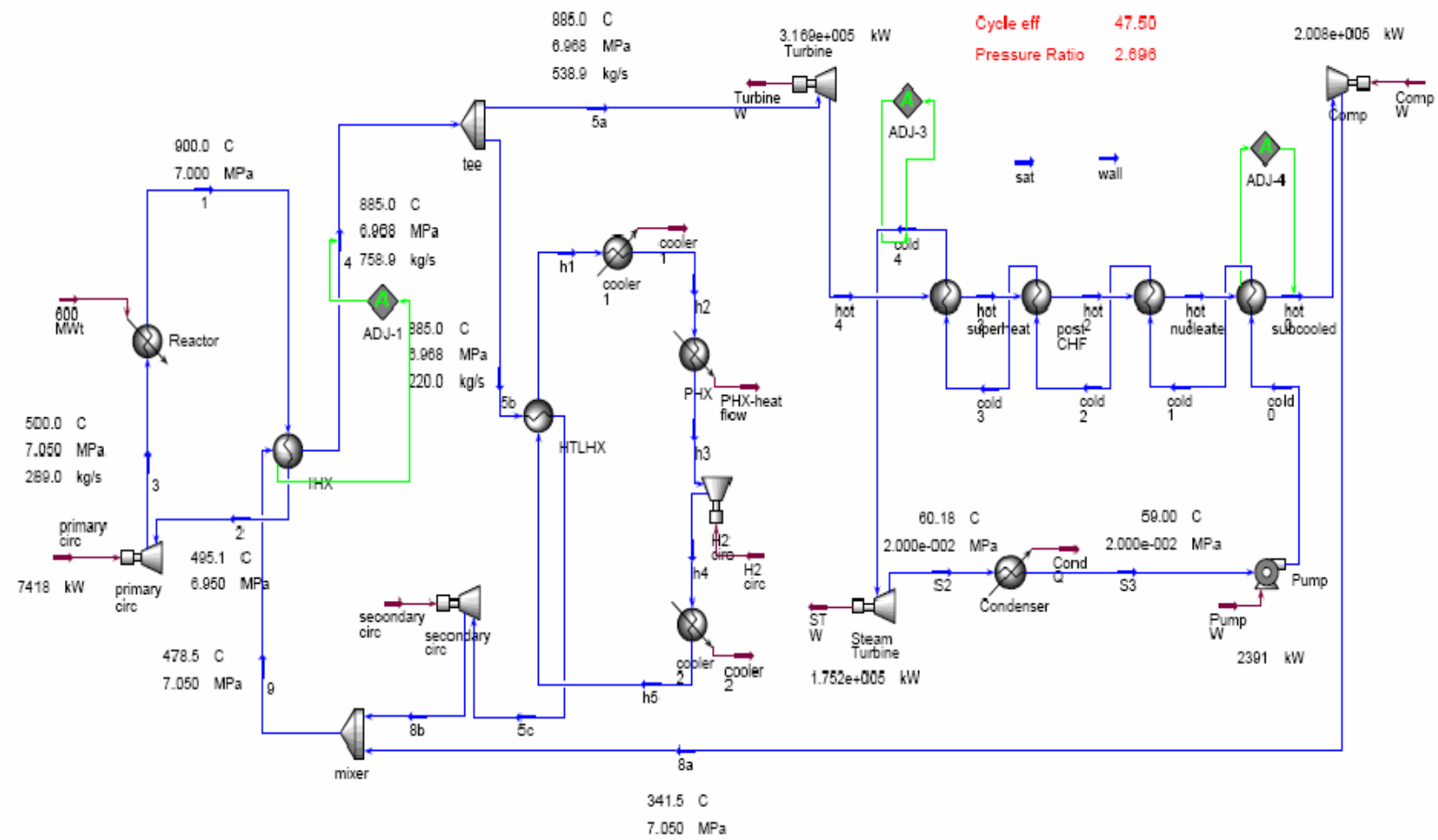

Figure 22. HYSYS diagram of Brayton top cycle with a nitrogen-helium mixture working fluid.

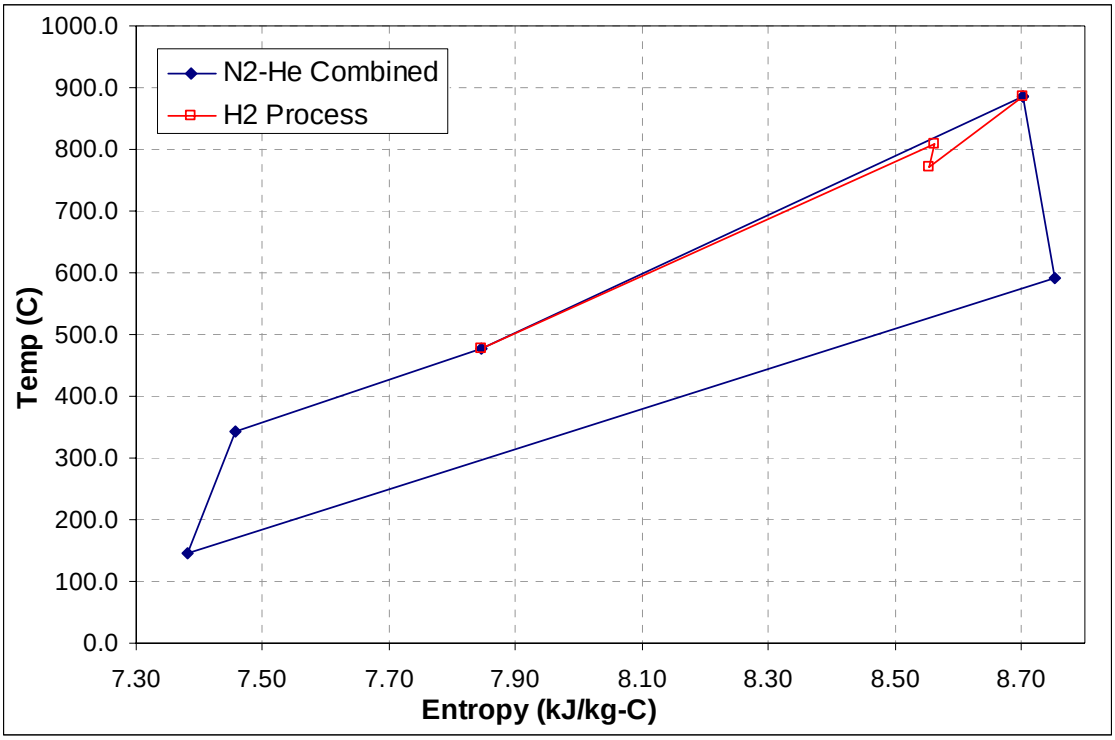

Figure 23. T-S diagram of Brayton top cycle with a nitrogen-helium mixture working fluid.

TABLE XIX
State points for Brayton top cycle with a nitrogen-helium mixture working fluid.

Point	Temp (°C)	Pressure (Mpa)	Entropy (kJ/kg-K)	Enthalpy (kJ/kg)
1	900.0	7.00	19.33	4561.1
2	495.1	6.95	17.15	2459.0
3	500.0	7.05	17.16	2484.7
4,5(a,b)	885.0	6.97	8.70	1670.4
5c	772.4	6.41	8.55	1446.2
6	592.2	2.67	8.75	1087.7
7	146.2	2.59	7.38	228.5
8a	341.4	7.05	7.46	604.5
8b	809.6	7.05	8.56	1520.6
9	478.5	7.05	7.85	870.1

TABLE XX
Component sizing data for combined cycle with a nitrogen-helium mixture.

Component	Value
Gas Turbine work (MW)	316.9
Steam Turbine work (MW)	175.2
Compressor work (MW)	200.8
Pump work (MW)	2.4
Circulator work (MW)	23.8
IHX volume (m^3)	71.7
HTLHX volume (m^3)	1.7
Steam generator volume (m^3)	130.4

4. Parametric Studies

Parametric studies were performed on the reactor outlet temperature, secondary mass flow rate, pressure, and turbine for the 3 working fluids. The results are summarized in Figure 24, Figure 25, Figure 26 and Table XXI. Increasing the reactor outlet temperature affected the fluids in different ways. Increasing from 850°C to 900°C had the largest effect on the nitrogen-helium mixture with an increase of 1.5% and the smallest effect on CO_2 with an increase of only 1%, with helium in the middle with an increase of 1.4%. Further increasing the reactor outlet temperature to 1000°C demonstrated a different trend with the CO_2 and nitrogen-helium mixture increasing by only 0.5% while the helium increased by 0.8%.

Decreasing the mass flow of the cycle had a larger impact on the helium and nitrogen-helium mixture than for the CO_2. In general as the mass flow was decreased the efficiency decrease for all fluids was amplified. Note that for the helium working fluid it started out 0.2% lower than that for the nitrogen-helium mixture but at lower mass flow rates the efficiencies are comparable.

The effects of pressure on the system are similar for all fluids. The trend shows that as the pressure is decreased from the amplitude of the efficiency decrease grows. The effect of turbine cooling on the system was an approximately 0.5% efficiency decrease for all working fluids.

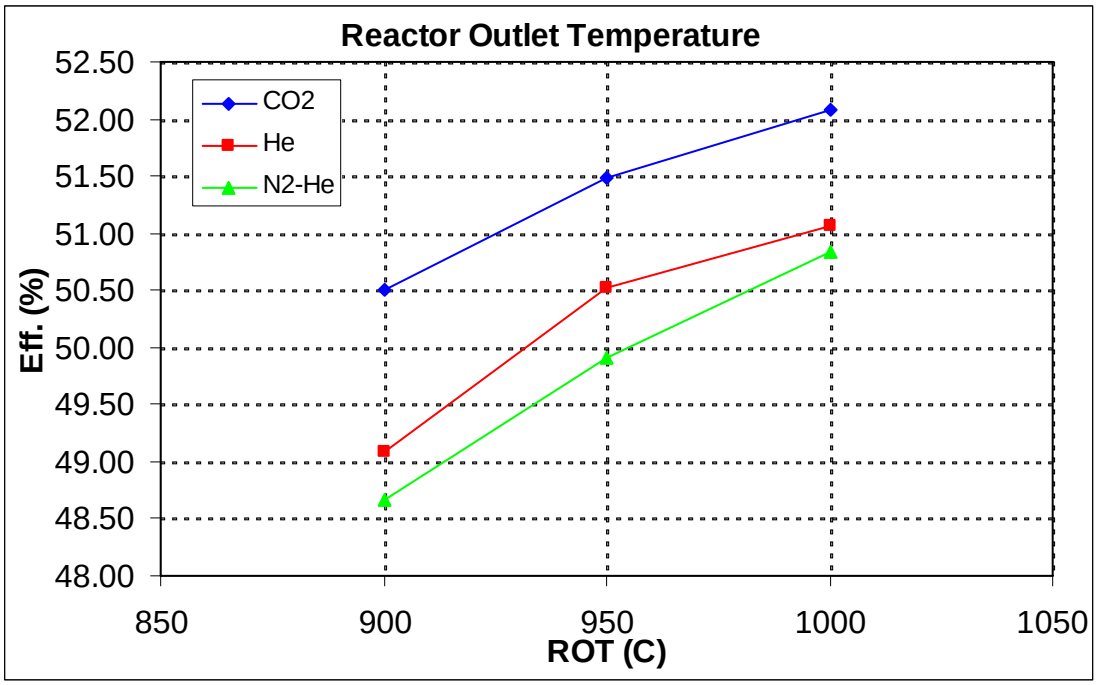

Figure 24. Parametric study of the effects of reactor outlet temperature on combined cycle efficiency.

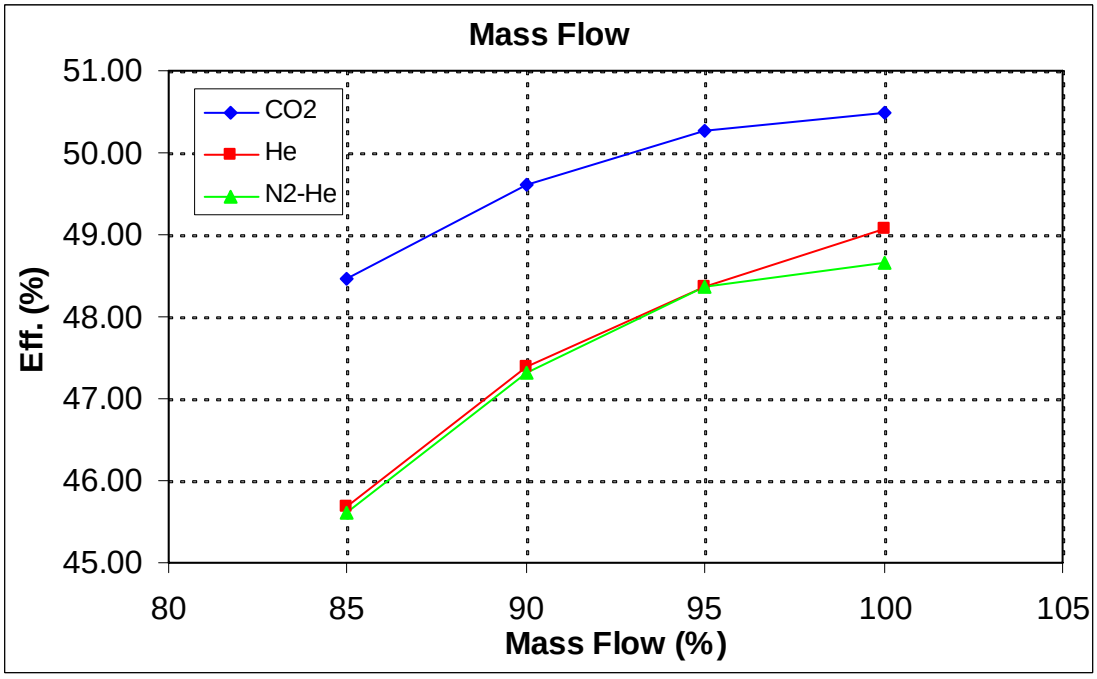

Figure 25. Parametric study of the effects of secondary mass flow rate on combined cycle efficiency.

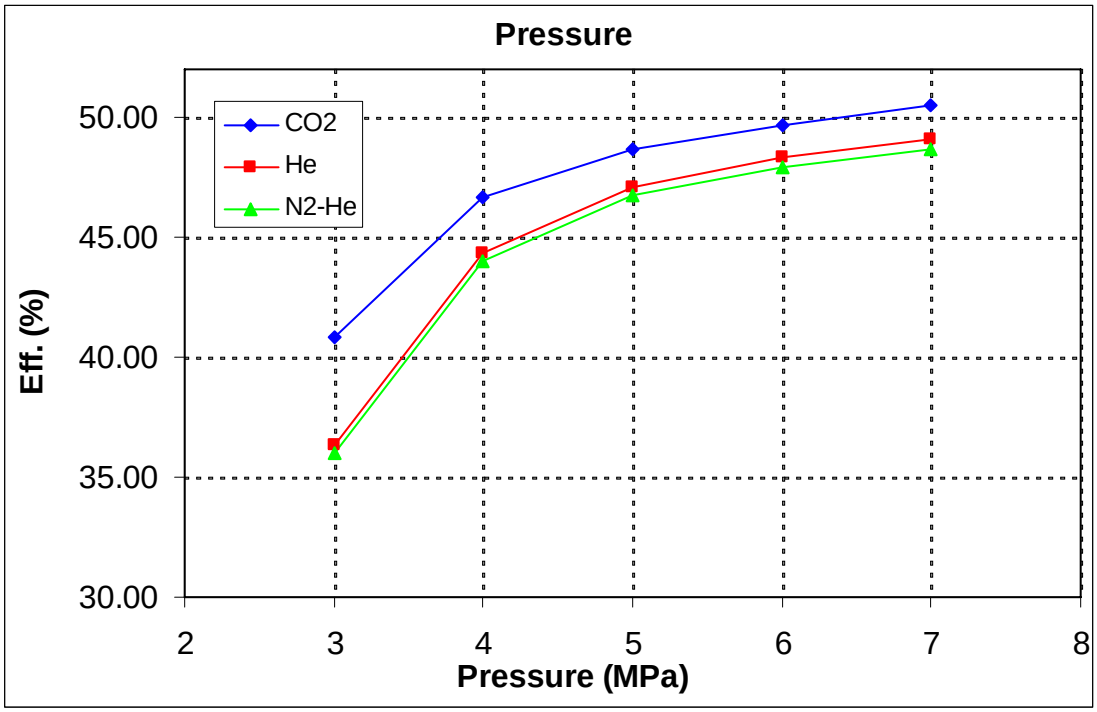

Figure 26. Parametric study of the effects of working pressure on combined cycle efficiency.

TABLE XXI
Parametric study of the effects of turbine cooling on combined cycle efficiency.

Turbine Cooling			
	CO2	**He**	**N2-He**
None	50.50	49.08	48.66
8%	50.26	48.83	48.42

C. Reheated Cycle

The reheat cycle, illustrated in Figure 6 consists of; (1) a primary loop with 4 IHX's (2) an intermediate heat transport loop in series with the IHX's on the primary loop, (3) the PCU with four turbines (high pressure turbine, medium pressure turbine 1, medium pressure turbine 2, low pressure turbine), 4 compressors (low pressure compressor, medium pressure compressor 1, medium pressure compressor 2, and high

pressure compressor) 1 precooler, 3 intercoolers and a recuperator. This cycle was simulated using flibe as the working fluid in the primary side and helium in the intermediate heat transport loop. Helium, CO_2 and the N_2-He mixture were simulated in the PCU and the results are described in Sections 1, 2 and 3, respectively.

Comparing the working fluids in this cycle, helium produces the highest efficiency. However, it also has largest heat exchangers and turbomachinery. Using the N_2-He mixture produces a slightly lower efficiency but with smaller heat exchangers. The CO_2 working fluid has a much lower, approximately 3%, cycle efficiency than the helium and N_2-He mixture; however, it has the smallest turbomachinery of all the fluids.

1. Helium Working Fluid

The helium working fluid was optimized for the reheated cycle with a pressure ratio of 4.433 and an efficiency of 57.42%. The secondary mass flow rate was optimized at 200 kg/s. The HYSYS simulation is illustrated in Figure 27, the T-S diagram is shown in Figure 29 and the state points are summarized in Table XXII. The total heat exchanger volume was 373.2 m^3 and the total cycle work was 729.6 MW. Table XXIII lists the individual component sizing results for the cycle.

A study was also performed on the helium cycle to verify the use of Flibe in the primary side in place of helium. Figure 28 shows the HYSYS simulation using a helium working fluid on the primary side. The efficiency of this cycle was 51.54% with a pressure ratio of 4.433. Comparing this to the three-shaft cycle, with an efficiency of 50.93%, there is only a .61% efficiency increase. This efficiency gain does not offset the cost of the additional complexity of the cycle. Therefore, using helium as a working fluid in the primary side was not a viable option and was not studied further.

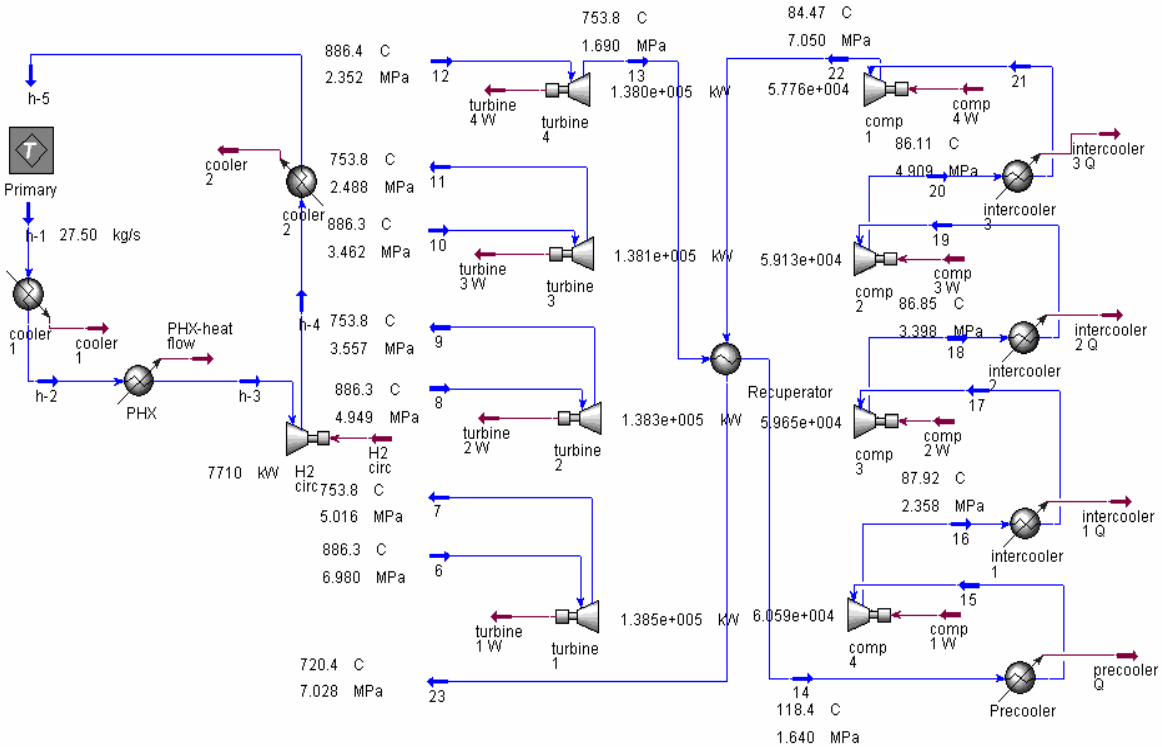

Figure 27. HYSYS diagram of the reheated configuration with helium working fluid.

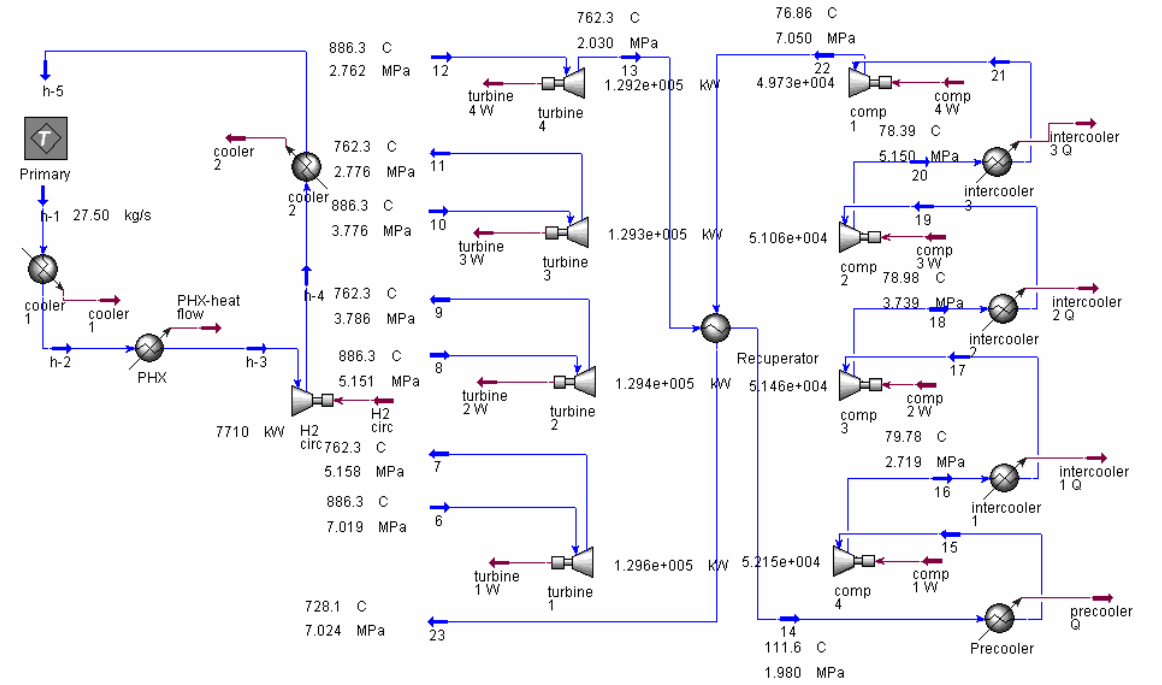

Figure 28. HYSYS diagram of the reheated configuration with helium working fluid on primary and secondary sides.

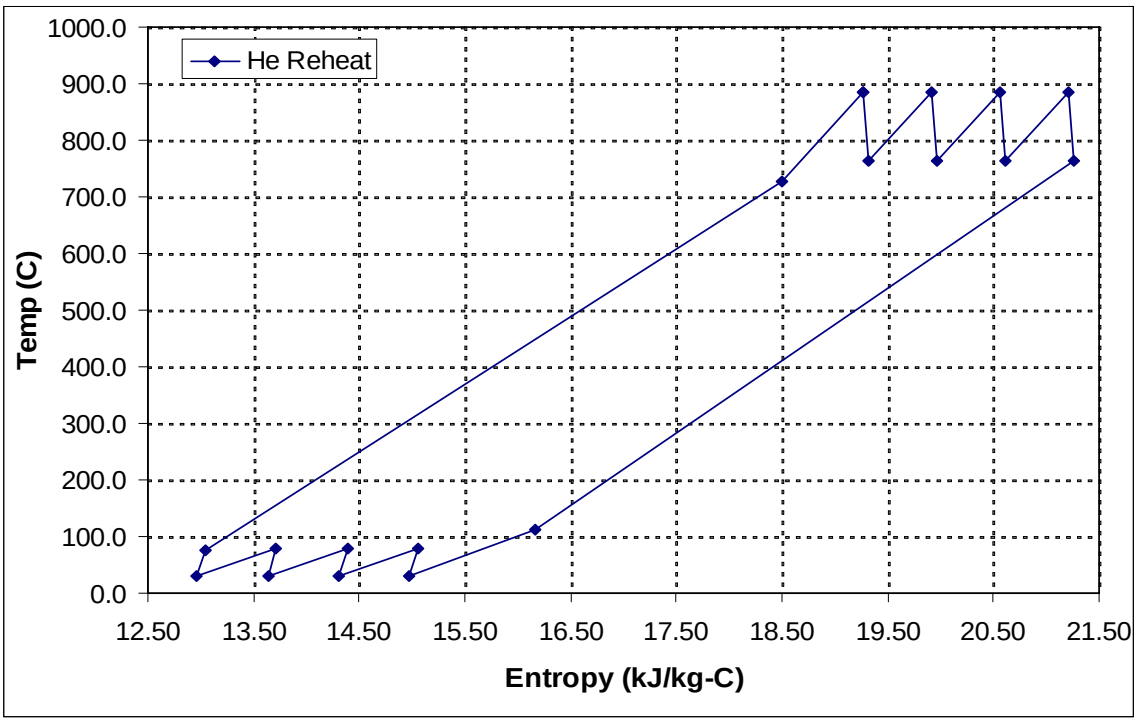

Figure 29. T-S diagram for the reheated configuration with helium working fluid.

TABLE XXII
State points for the reheated configuration with helium working fluid.

Point	Temp (°C)	Pressure (MPa)	Entropy (kJ/kg-K)	Enthalpy (kJ/kg)
1	900.0	0.1013	-10.40	-7374.1
2	900.0	0.1013	-10.40	-7374.1
3a	744.6	0.1013	-11.29	-7744.8
3b	778.7	0.1013	-11.09	-7663.4
3c	778.7	0.1013	-11.09	-7663.4
3d	778.7	0.1013	-11.09	-7663.4
3h	559.4	0.1013	-12.56	-8186.5
4	763.3	0.1013	-11.18	-7700.3
5	763.3	0.1013	-11.18	-7700.3
6	886.3	7.02	19.27	4490.0
7	762.3	5.16	19.32	3842.0
8	886.3	5.15	19.91	4486.0
9	762.3	3.79	19.96	3839.0
10	886.3	3.78	20.55	4483.1
11	762.3	2.78	20.61	3836.8
12	886.3	2.76	21.20	4481.0

TABLE XXII continued.

Point	Temp (°C)	Pressure (MPa)	Entropy (kJ/kg-K)	Enthalpy (kJ/kg)
13	762.3	2.03	21.25	3835.2
14	111.6	1.98	16.16	455.3
15	30.0	1.93	14.98	31.4
16	79.8	2.72	15.06	292.1
17	30.0	2.67	14.31	33.4
18	79.0	3.74	14.39	290.7
19	30.0	3.69	13.64	36.3
20	78.4	5.15	13.71	291.6
21	30.0	5.10	12.97	40.2
22	76.9	7.05	13.04	288.8
23	728.1	7.02	18.51	3668.8

TABLE XXIII
Component sizing data for reheated cycle with helium working fluid.

Component	Value
Turbine work (MW)	517.5
Compressor work (MW)	204.4
Circulator work (MW)	7.7
IHX volume (m^3)	247.0
HTLHX volume (m^3)	4.7
Recuperator volume (m^3)	121.6

2. CO_2 Working Fluid

The CO_2 working fluid was optimized for the reheated cycle with a pressure ratio of 10.77 and a PCU efficiency of 53.72%. The secondary mass flow rate was optimized at 1050 kg/s. The HYSYS simulation is illustrated in Figure 30, the T-S diagram is shown in Figure 31 and the state points are summarized in Table XXIV. The total heat exchanger volume was 354.6 m^3 and the total cycle work was 615.3 MW. Table XXV lists the individual component sizing results for the cycle.

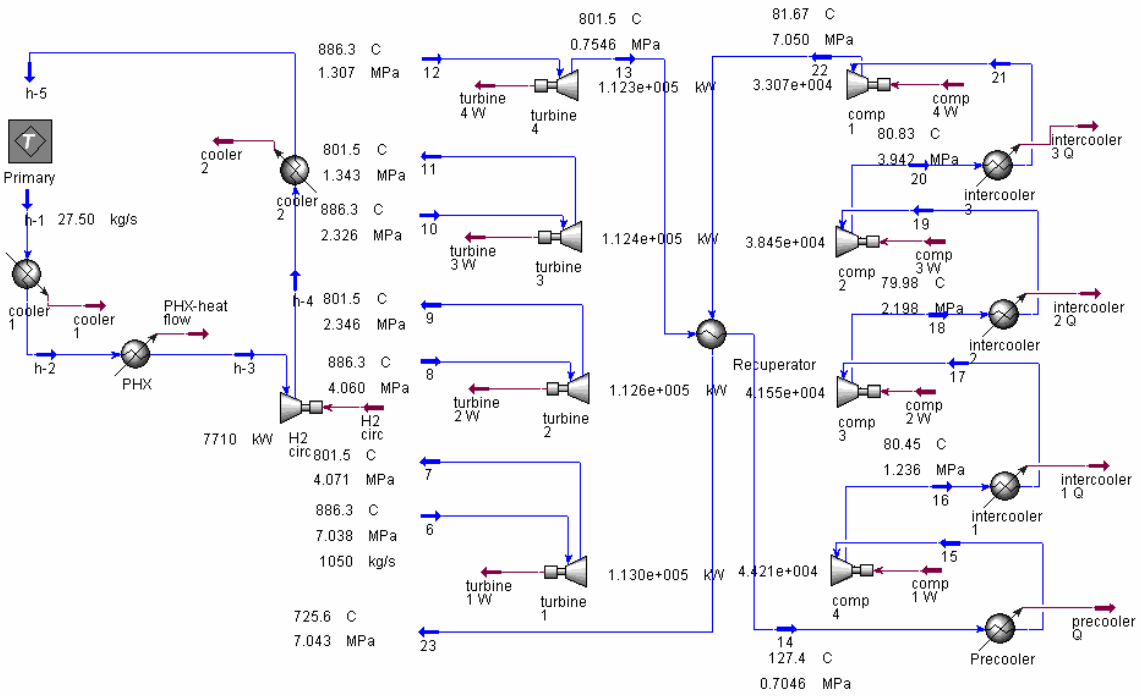

Figure 30. HYSYS diagram of the reheated configuration with CO_2 working fluid.

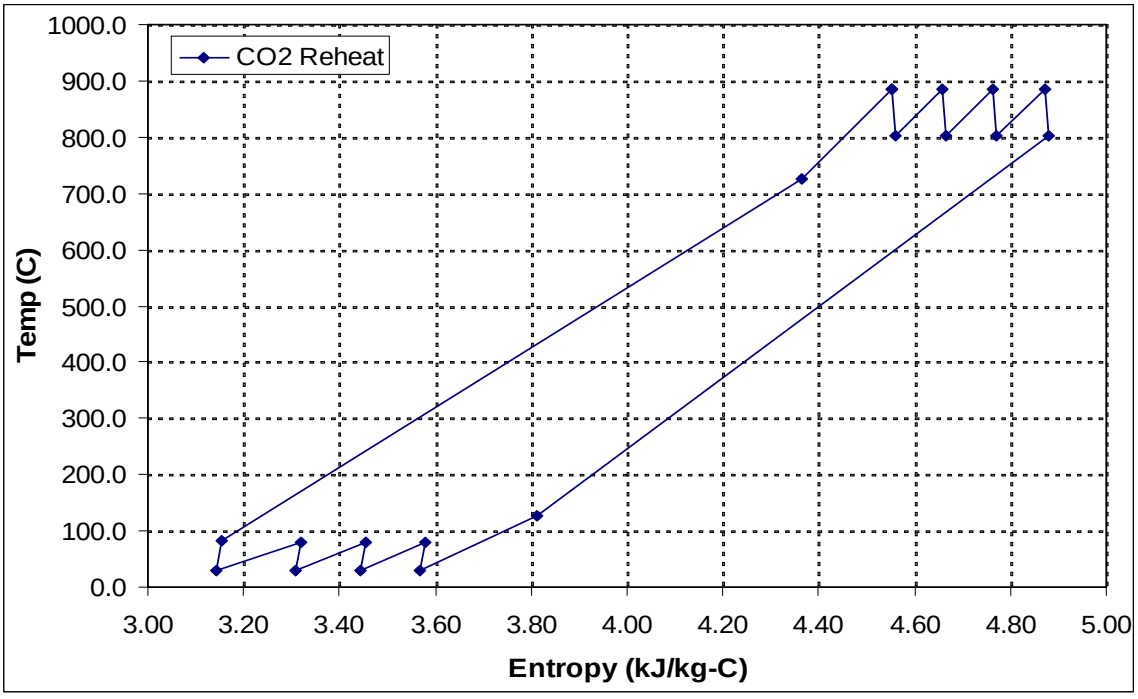

Figure 31. T-S diagram of the reheated configuration with CO_2 working fluid.

TABLE XXIV
State points for the reheated configuration with CO2 working fluid.

Point	Temp (°C)	Pressure (Mpa)	Entropy (kJ/kg-K)	Enthalpy (kJ/kg)
1	900.0	0.1013	-10.40	-7374.1
2	900.0	0.1013	-10.40	-7374.1
3a	742.9	0.1013	-11.30	-7748.8
3b	818.1	0.1013	-10.85	-7569.4
3c	818.1	0.1013	-10.85	-7569.4
3d	818.2	0.1013	-10.85	-7569.3
3h	559.4	0.1013	-12.56	-8186.5
4	793.3	0.1013	-11.00	-7628.5
5	793.3	0.1013	-11.00	-7628.5
6	886.3	7.04	4.55	-7997.3
7	801.5	4.07	4.56	-8104.9
8	886.3	4.06	4.66	-7997.5
9	801.5	2.35	4.67	-8104.7
10	886.3	2.33	4.76	-7997.6
11	801.5	1.34	4.77	-8104.6
12	886.3	1.31	4.87	-7997.6
13	801.5	0.75	4.88	-8104.5
14	127.4	0.70	3.81	-8859.1
15	30.0	0.65	3.57	-8949.6
16	80.4	1.24	3.58	-8907.5
17	30.0	1.19	3.44	-8954.8
18	80.0	2.20	3.46	-8915.2
19	30.0	2.15	3.31	-8964.9
20	80.8	3.94	3.32	-8928.3
21	30.0	3.89	3.14	-8986.3
22	81.7	7.05	3.15	-8954.8
23	725.6	7.04	4.36	-8200.2

TABLE XXV
Component sizing data for reheated cycle with CO_2 working fluid.

Component	Value
Turbine work (MW)	450.3
Compressor work (MW)	157.3
Circulator work (MW)	7.7
IHX volume (m^3)	218.1
HTLHX volume (m^3)	4.7
Recuperator volume (m^3)	131.8

3. Nitrogen-Helium Working Fluid

The N_2-He mixture was optimized for the reheated cycle with a pressure ratio of 3.87 and a PCU efficiency of 57.13%. The secondary mass flow rate was optimized at 600 kg/s. The HYSYS simulation is illustrated in Figure 32, the T-S diagram is shown in Figure 33 and the state points are summarized in Table XXVI. The total heat exchanger volume was 286.8 m^3 and the total cycle work was 717.9 MW. Table XXVII lists the individual component sizing results for the cycle.

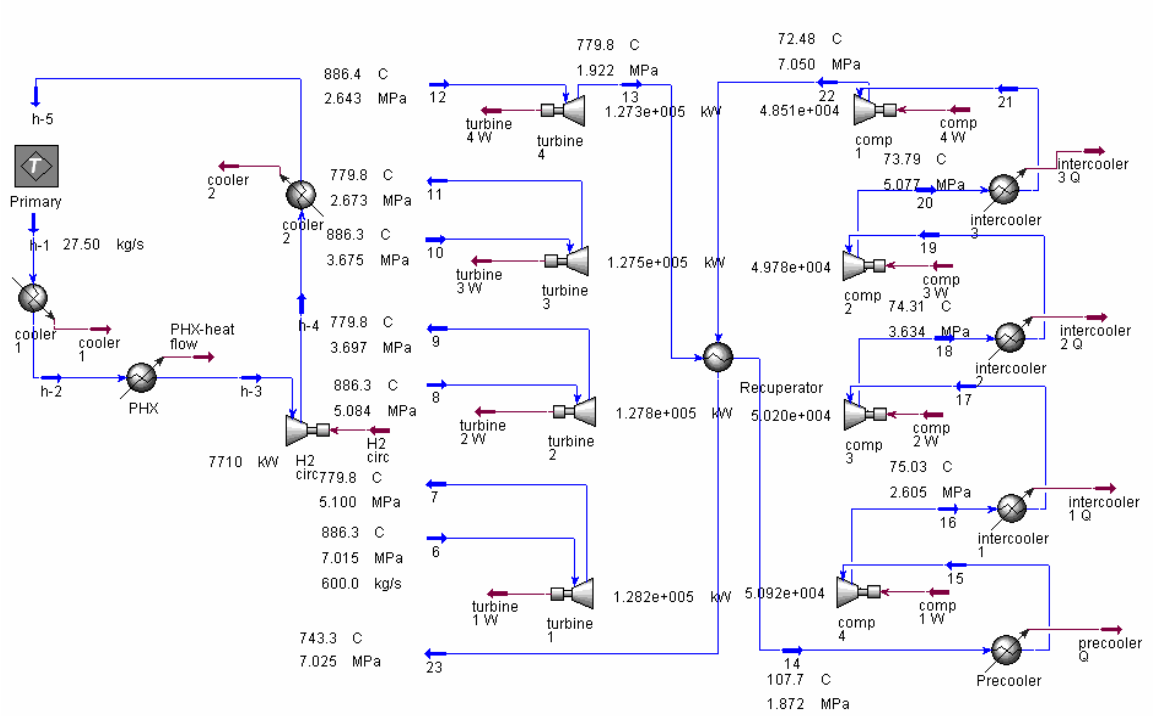

Figure 32. HYSYS diagram of the reheated configuration with a nitrogen-helium mixture working fluid.

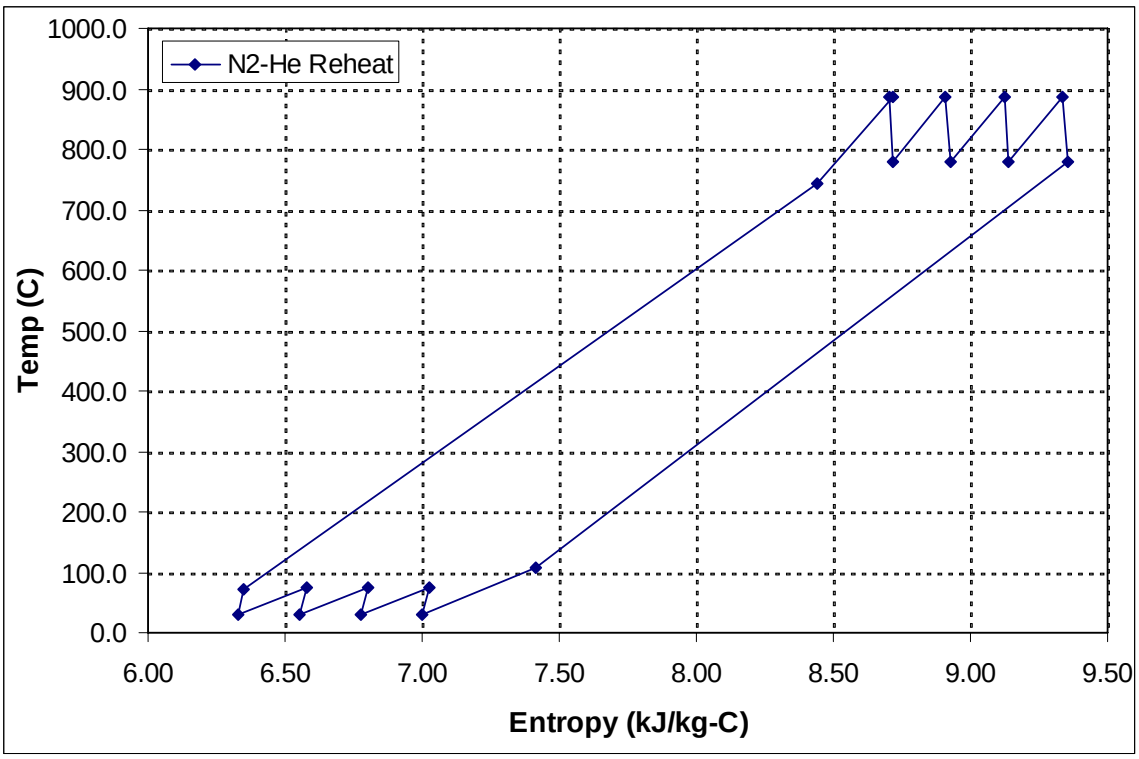

Figure 33. T-S diagram of the reheated configuration with a nitrogen-helium mixture working fluid.

TABLE XXVI
State points for the reheated configuration with a nitrogen-helium mixture working fluid.

Point	Temp (°C)	Pressure (Mpa)	Entropy (kJ/kg-K)	Enthalpy (kJ/kg)
1	900.0	0.1013	-10.40	-7374.1
2	900.0	0.1013	-10.40	-7374.1
3a	759.9	0.1013	-11.20	-7708.3
3b	796.3	0.1013	-10.98	-7621.4
3c	796.3	0.1013	-10.98	-7621.4
3d	796.4	0.1013	-10.98	-7621.1
3h	559.4	0.1013	-12.56	-8186.5
4	780.7	0.1013	-11.07	-7658.6
5	780.7	0.1013	-11.07	-7658.6
6	886.3	7.02	8.70	1673.1
7	779.8	5.10	8.72	1459.4
8	886.3	5.08	8.91	1670.7
9	779.8	3.70	8.93	1457.8
10	886.3	3.68	9.12	1669.0
11	779.8	2.67	9.14	1456.6
12	886.4	2.64	9.34	1668.0
13	779.8	1.92	9.35	1455.7
14	107.7	1.87	7.41	155.3
15	30.0	1.82	7.00	8.8
16	75.0	2.61	7.02	93.6
17	30.0	2.56	6.78	8.6
18	74.3	3.63	6.80	92.2
19	30.0	3.58	6.55	8.3
20	73.8	5.08	6.58	91.3
21	30.0	5.03	6.33	8.0
22	72.5	7.05	6.35	88.9
23	743.3	7.03	8.44	1389.3

TABLE XXVII
Component sizing data for reheated cycle with a nitrogen-helium mixture working fluid.

Component	Value
Turbine work (MW)	510.8
Compressor work (MW)	199.4
Circulator work (MW)	7.7
IHX volume (m^3)	153.1
HTLHX volume (m^3)	4.7
Recuperator volume (m^3)	129

D. Effects of IHTL and HTSE

The HTSE plant was coupled to the reactor and power conversion unit by means of the intermediate heat transport loop. Helium and molten salt were investigated as working fluids in the IHTL.

Figure 34 depicts the HYSYS simulation of the entire plant including a 3-Shaft PCU and the HTSE plant. Using Equation 2 the overall efficiency was calculated for the various PCU and IHTL working fluids, and PCU configurations. Table XXVIII summarizes the overall efficiency of the plant for the various configurations and working fluids. The overall efficiency of the facility is ~4-5% lower than the PCU efficiency. This is due to the addition of the pumping power in the IHTL and HTSE.

The HTSE facility requires electrical power from the PCU to operate the electrolysis cell. Therefore much of the electrical power produced by the PCU is required by the HTSE. The excess power from the PCU can be used for electrical generation. The amount of excess power available for electrical generation varies for each configuration. Table XXIX summarizes the electrical power generation for each configuration. When using a helium working fluid in the IHTL, hydrogen can be produced at a rate of 113.7 kg/hr, while using the molten salt working fluid produces 96.42 kg/hr of hydrogen. The difference in these values is due to the amount of heat that is being transferred to the HTSE facility by the working fluids. This is due to the assumptions made in the design of the IHTL. The amount of hydrogen produced can be adjusted by increasing the heat flow through the IHTL and increasing the electrical power sent to the electrolysis cell. These are competing values, as the heat transfer to the IHTL increases the power to PCU and electrical generation decreases.

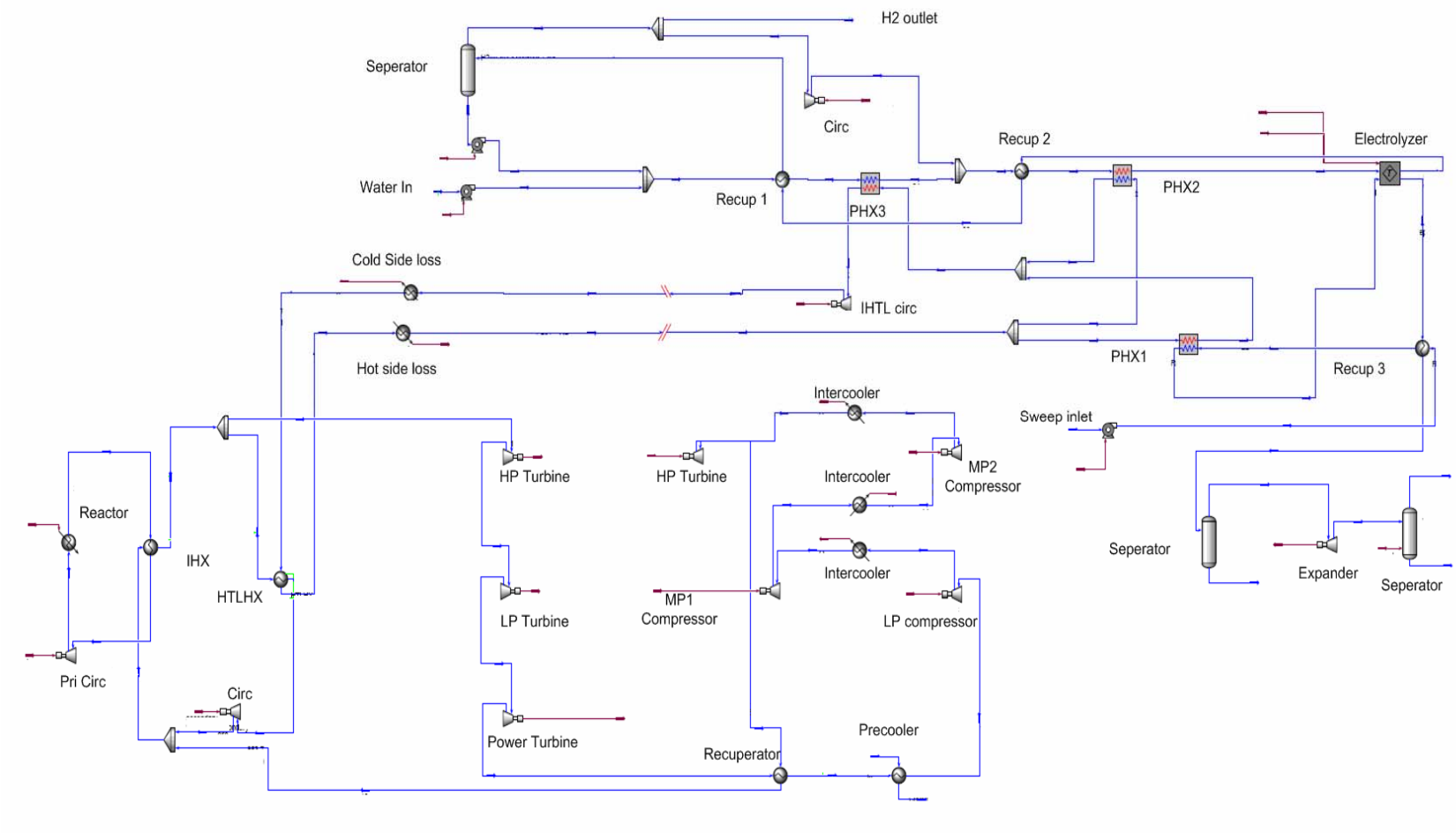

Figure 34. HYSYS model of entire plant with a 3-shaft PCU and HTSE plant.

TABLE XXVIII
Summary of overall plant efficiency for each PCU configuration and IHTL working fluid.

PCU configuration and working fluid	Efficiency (Helium)	PCU configuration and working fluid	Efficiency ($NaBF_4$-NaF)
3-Shaft		3-Shaft	
He	44.83	He	46.02
CO2	41.09	CO2	42.26
N2-He	44.78	N2-He	45.94
Combined		Combined	
He	43.07	He	44.40
CO2	44.35	CO2	45.69
N2-He	42.69	N2-He	44.02
Reheat		Reheat	
He	50.80	He	51.99
CO2	47.45	CO2	48.64
N2-He	50.52	N2-He	51.71

TABLE XXIX
Excess power available for electrical generation for each PCU configuration and IHTL working fluid.

PCU configuration and working fluid	Electrical Power (Helium)	PCU configuration and working fluid	Electrical Power ($NaBF_4$-NaF)
3-Shaft	MW	3-Shaft	MW
He	43.29	He	84.62
CO2	20.87	CO2	62.07
N2-He	42.97	N2-He	84.12
Combined		Combined	
He	32.71	He	74.91
CO2	40.43	CO2	82.63
N2-He	30.45	N2-He	72.65
Reheat		Reheat	
He	79.13	He	120.45
CO2	59.03	CO2	100.35
N2-He	77.43	N2-He	118.75

IV. CONCLUSIONS

The commercial process code HYSYS has been used to produce a complete balance of plant for the NGNP project including a reactor in an indirect cycle coupled to a PCU and to a HTSE by means of the IHTL. Several PCU configurations including a three-shaft, combined and reheated cycle were model. Efficiency data for these three configurations as well and the entire plant efficiency were obtained. Component sizing data was produced for the PCU turbomachinery and heat exchangers. Finally parametric studies away from the baseline design on the three-shaft and combined cycle were performed to determine the effects of reactor outlet temperature, PCU mass flow rate, PCU operating pressure and turbine cooling.

In the three-shaft cycle helium had the best PCU efficiency of 50.93%. The nitrogen-helium mixture gave a slightly lower cycle efficiency of 50.76%. CO_2 had a much lower cycle efficiency at 46.73%. The turbomachinery work using CO_2 was approximately 8.8% lower than the work when using helium and the mixture. Dostal et al. (2004) also states that for turbomachinery of the same power, CO_2 is much smaller than that of helium. The nitrogen helium mixture produced the smallest total heat exchanger volume followed by helium and then CO_2. Although the heat exchanger volume is larger for CO_2 the total cost of the plant could be less than that of a He or nitrogen-helium mixture due to its smaller turbomachinery size. Parametric studies demonstrated that helium is less susceptible to changes in working conditions than CO_2 and the nitrogen-helium mixture. The advantage of this is reduced losses during off normal operations; however if the reactor were to be up rated to a higher outlet temperature the increase in efficiency would not be as advantageous as for the other working fluids. The nitrogen-helium mixture is recommended for use in the three-shaft design due to its high efficiency and small heat exchanger volumes. Helium is not recommended due to its large heat exchangers. CO_2 is not recommended due to its low efficiency.

For the combined cycle CO_2 proved to be the best working fluid in terms of efficiency, with an efficiency of 50.50%. Helium had an efficiency of 49.10% and the nitrogen-helium mixture had an efficiency of 48.70%.The turbomachinery work using CO_2 was approximately 8.5% lower than the work when using helium and the mixture. CO_2 models showed a total heat exchanger size slightly higher than that of the helium. The total heat exchanger volume for the combined cycle is the lowest of all the PCU configurations. It also uses existing steam cycle technology making it a very attractive candidate. Parametric studies demonstrated that the various working fluids were affected differently by the working conditions within the cycle. The pressure study also highlighted that the combined cycle was not greatly effected by the pressure. Therefore, lower pressures could be used in the system to decrease component sizes with a small decrease in efficiency. Due to its small dependence on working conditions such as pressure and smaller heat exchanger sizes as compared to the 3-shaft cycle, the combined cycle is recommended. Further exploration of this cycle could include improvements to the steam cycle efficiency by the use of feed water heaters and reheating. CO_2 is recommended for the combined cycle due to its high efficiency and small component sizes.

Finally the helium working fluid has the best PCU efficiency of 57.42% for the reheated cycle. The nitrogen-helium mixture gave a slightly lower efficiency of 57.13% and CO_2 had a much lower efficiency at 53.72%. The turbomachinery work using CO_2 was approximately 15.2% lower than the work when using helium and the mixture. The nitrogen helium mixture produced the smallest total heat exchanger volume followed by CO_2 and then helium. A study using helium as the primary working fluid gave an efficiency of 51.54%. Comparing this to the 3-shaft option efficiency of 50.93 confirms that the use of helium as the primary working fluid is not a viable option. The reheat option allows for increased efficiency; however the complexity and construction costs are amplified. The total heat exchanger volume is approximately 50% larger than that for the combined cycle. The nitrogen-helium mixture is recommended for use in the reheated cycle due to its high efficiency and small heat exchanger volumes. Helium is not

recommended due to its large heat exchangers. CO_2 is not recommended due to its low efficiency.

The use of an intermediate heat transport and high-temperature steam electrolysis plant allows the production of hydrogen and electricity. With approximately 50MW of process heat being transferred to the HTSE facility hydrogen can be produced at a rate of 96.42 to 113.7 kg/hr. The use of a molten salt in the IHTL increases the overall cycle efficiency by 1-2% lowering the pumping power required in the loop. The electrical power generated by the PCU must be used to power the electrolysis cell. In doing this the net electrical output is decreased.

REFERENCES

1. ENERGY INFORMATION ADMINISTRATION, June 2006, "New Reactor Designs," available on the internet at <www.eia.doe.gov/cneaf/nuclear/page/analysis/nucenviss2.html>

2. C. DAVIS, C. OH, R. BARNER, S. SHERMAN and D. WILSON, "Thermal-Hydraulic Analyses of Heat Transfer Fluid Requirements and Characteristics for Coupling a Hydrogen Production Plant to a High-Temperature Nuclear Reactor," INL/EXT-05-00453, Idaho National Laboratory (2005).

3. ANWL, "Reactor/Process Interface Requirements," ANWL7500-0001-ES-00 Argonne National West Laboratory (2004).

4. I. SOCHET, J. L. ROUYER, and P. HEMMERICH, 2004, "Safe Hydrogen Generation by Nuclear HTR," Paper 4261, *Proceedings of ICAPP '04*, Pittsburgh, PA, USA (June 13-17, 2004).

5. C. SMITH, S. BECK, and B. GALYEAN, "An Engineering Analysis for Separation Requirements of a Hydrogen Production Plant and High-Temperature Nuclear Reactor," INL/EXT-05-00137 Rev 0, Idaho National Laboratory (2005).

6. C. B. BAXI, E. PEREZ, A. SHENOY, V.I. KOSTON, N.G. KODOCHIGOV, A.V. VASYAEV, S.E. BELOV and V.F. GOLOVKO, "Evolution of the Power Conversion Unit Design of the GT-MHR," Paper 6213, *Proceedings of ICAPP '06* Reno, NV June 4-8 (2006).

7. B. COPSEY, M. LECOMTE, G. BRINKMANN, A. CAPITAINE, and N. DEBERNE, "The Framatome ANP Indirect-Cycle Very High Temperature Reactor," Paper 4201, *Proceedings of ICAPP '04*, Pittsburg, PA , June 13-17 (2004).

8. P. F. PETERSON, "Multiple-Reheat Brayton Cycles for Nuclear Power Conversion with Molten Coolants," *Nuclear Technology*, **144**, 279 (2002).

9. C.M. STOOTS, J.E. O'BRIAN, M.G. MCKELLAR, and G.L. HAWKES, "Engineering Process Model for High-Temperature Electrolysis System Performance Evaluation," Internal Report, Idaho National Laboratory (2005).

10. INDEPENDENT TECHNOLOGY REVIEW GROUP, "Design Features and Technology Uncertainties for the Next Generation Nuclear Plant," INEEL/EXT-04-01816, Idaho National Engineering and Environmental Laboratory (2004).

11. INEEL, "Next Generation Nuclear Plant Research and Development Program Plan," INEEL/EXT-05-02581, Idaho National Engineering and Environmental Laboratory (2005).

12. P.E. MACDONALD, J.W. STERBENTZ, R.L. SANT, P.D. BAYLESS, R.R. SCHULTZ, H.D. GOUGAR, R.L. MOORE, A.M. OUGOUAG and W.K. TERRY, "NGNP Preliminary Point Design – Results of the Initial Neutronics and Thermal-hydraulic Assessments," INEEL/EXT-03-00870, Idaho National Engineering and Environmental Laboratory (2003).

13. C. OH and R. BARNER, "Effects of Interstage Cooling on Brayton Cycle Efficiency," *Proceedings of ANS Annual Meeting*, Reno, NV, June 4-8 (2006).

14. V. DOSTAL, J. M. DRISCOLL, and P. HEJZLAR, "A Supercritical Carbon Dioxide Cycle for Next Generation Nuclear Reactors," MIT-ANP-TR-100, Massachusetts Institute of Technology (2004).

15. J.E. O' BRIAN, C. M. STOOTS, and G.L. HAWKES, "Comparison of a One-Dimensional Model of a High-Temperature Solid-Oxide Electrolysis Stack with CFD and Experimental Results," *Proceedings of 2005 ASME International Mechanical Engineering Congress and Exposition IMECE2005*, Orlando, FL (2005).

16. R. PERRY, D. GREEN and J. MALONEY, *Perry's Chemical Engineer's Handbook,* Sixth Edition, McGraw- Hill, New York, NY (1984).

17. ASPEN TECHNOLOGY, "HYSYS Simulation Basis Manual," available on the internet at <www.aspentech.com> (2006).

18. NATIONAL INSTITUTE OF STANDARDS, "Thermophysical Properties of Fluid Systems", available on the internet at <webbook.nist.gov/chemistry/fluid/> (2006).

19. HEATRIC, "PHCE design", available on the internet at <www.heatric.com> (2006).

20. IDAHO NATIONAL LAB, *RELAP5-3D Code Manuals*, Revision 2.3, Idaho National Laboratory, Idaho Falls, ID (2006).

21. W.M. KAYES and M.E. CRAWFORD, "Convective Heat and Mass Transfer," Second Edition, McGraw-Hill, New York, NY (1980).

22. P.E. MACDONALD and J. BUONGIORNO, "Design of an Actinide Burning, Lead or Lead-Bismuth Cooled Reactor that Produces Low Cost Electricity," INEEL/EXT-02-01249, Idaho National Engineering and Environmental Laboratory (2002).

23. R.B. BIRD, W.E. STEWART and E.N. LIGHTFOOT, *Transport Phenomena*, John Wiley & Sons, Inc., New York, NY (1960).

24. J.G. COLLIER and J.R. THOME, *Convective Boiling and Heat Transfer*, Third Edition, Oxford University Press, Oxford (1994).

25. N.E. TODREAS and M.S. KAZIMI, *Nuclear Systems I: Thermal Hydraulic Fundamentals*, Hemisphere Publishing Co., Bristol, PA (1990).

26. "Generation IV Roadmap, Description and Evaluation of Candidate Gas-cooled Reactor Systems", TWG-2, Summary PRT XR01-03, Idaho National Engineering and Environmental Laboratory (2003).

27. H. SARAVANAMUTTOO, *Gas Turbine Theory*, Fifth Edition, Prentice Hall, New York, NY (1996).

VITA

Name:	Robert Buckner Barner
Address:	Department of Nuclear Engineering, Texas A&M University, 3133 TAMU, College Station, TX 77843-3133
Email Address:	rbbarner@gmail.com
Education:	B.S., Nuclear Engineering, Texas A&M University, 2004 M.S., Nuclear Engineering, Texas A&M University, 2006